

Personal Project Portfolio

Neeraj Kumar

Project Scientist

IIT delhi



July 9, 2025

Contents

1	Introduction	6
2	Project 1: Fatigue hotspot mitigation	6
2.1	Problem definition	6
2.2	Flowchart of the process	8
2.3	Stress tensor extraction and SN curve	10
2.4	Relation between SN curve and Load-time series	11
2.5	Design Iterations for Bottom cross (BC)	12
2.6	Summary	14
3	Project 2: Weld extrapolation for toe failure	15
3.1	Problem definition	15
3.2	Flowchart of the process	16
3.3	Weld extrapolation for Toe failure	17
3.4	Weld extrapolation for root failure	18
3.5	Neuber strain	19
3.6	Summary	22
4	Bolted joint verification	23
4.1	Problem definition	23
4.2	Flowchart of the process	25
4.3	Beam force extraction	26
4.4	Calculation of the Joint stiffness factor/Load factor Φ	27
4.5	Tension resistance calculation	31
4.6	Summary	32
5	Buckling analysis	33
5.1	Problem definition	33
5.2	Design Buckling resistance, $\alpha_{b,Rd}$	33

6 Fracture mechanics	38
6.1 Problem definition	38
6.2 Calculation of SCF K_t	38
6.3 Fracture toughness and fatigue tool	40
7 FSI experiment of Thermal power plant chimney	42
7.1 Problem definition/Objective	42
7.2 Methodology	42
7.3 Strain gauge installation in full bridge arrangement	43
7.4 Details of instrumentation and data recording	44
7.5 Calibration of gauges	45
7.6 Natural frequency and damping ratio experiment	46
7.7 Configurations for data recording	47
7.8 Result/Summary	47

List of Figures

1	Position of bottom cross GM	7
2	Geometry of Bottom cross	8
3	SN curve details	8
4	Fatigue mitigation process Flowchart	9
5	SN curve for different DC category	10
6	First iteration for Bottom cross	11
7	Load-time series and SN curve	11
8	Second iteration for Bottom cross	12
9	Third iteration for Bottom cross	13
10	Fourth iteration Bottom cross	13
11	Global model GM	15
12	Detail of the hotspot around lifting pins	15
13	Weld extrapolation Process Flowchart	17
14	Type "a" and type "b" classification by IIW	17
15	Type "a" and type "b" extrapolation	18
16	Extrapolation for root failure	19
17	Neuber strain	19
18	Weld hotspot near plates in GM	20
19	Fillet welds and extrapolation paths	21
20	Calculation spreadsheet	21
21	Nacelle RearFrame	23
22	Nacelle RearFrame	24
23	Process Flowchart	25
24	Beam connection shown	26
25	Axial and shear force from Beam	26
26	Bolt joint loading diagram under preload	27
27	Bolt joint diagram under axial load	28
28	Pressure cone	29

29	Static sliding between two plates	30
30	Load Multiplier from EC-3	33
31	Load Multiplier Eigen-Value Buckling	34
32	Max compression force on channel/Beam	35
33	Moment of inertia	35
34	Buckling Curves	36
35	Geometry of plate with hole	38
36	Maximum principal stress	39
37	Goodman mean stress correction	40
38	Fatigue tool settings	40
39	Tensile loading: Mode I	41
40	Elliptical crack	41
41	Stress intensity factor K_I	42
42	Plan and Elevation of the 1.6mx1.6m x9.6m Closed Circuit Wind Tunnel	43
43	The calibration of weights on the chimney	44
44	The calibration of weights on the chimney	45
45	The response from gauges in LabView	45
46	The response and Natural frequency	46
47	Amplitude Vs Time response	46
48	Two configuration for our experiment	47
49	Responses of gauge in loaded condition	48
50	Bending moment and Shear force	48

1 Introduction

In this portfolio I am showcasing few projects that I have worked on, with general understanding of physics and is intended to elaborate my skills and domains of expertise in structural analysis, Computational fluid dynamics and Product development of structural components.

2 Project 1: Fatigue hotspot mitigation

2.1 Problem definition

This problem concerns with fatigue mitigation for the component named Bottom cross (BC) in Rear Frame (RF), the Global model (GM) with position of BC and geometry of BC is shown in Figure 1 and Figure 2.

For fatigue evaluation I use cyclic loading in terms of linear accelerations, rotational velocities and rotational accelerations in X,Y,Z and apply these loads to the RF for evaluating the fatigue hotspots, the magnitude of these loads is in unit quantity and I call them Unit load case (ULC).

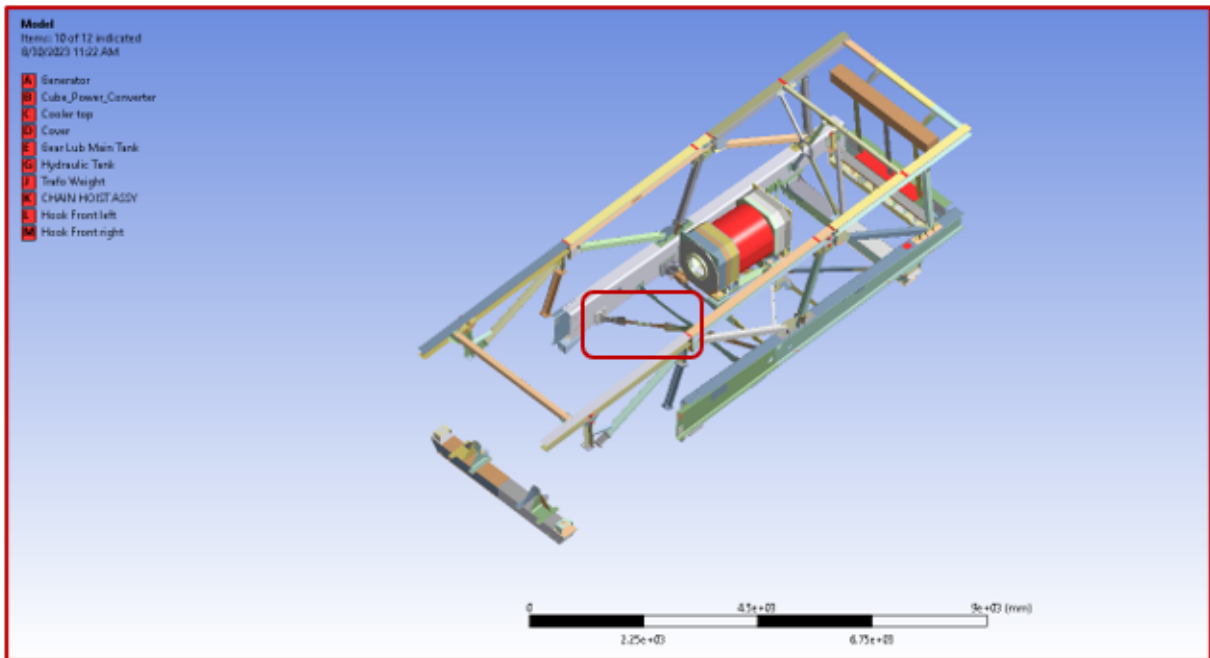


Figure 1: Position of bottom cross GM

As the component goes into tension-compression cycles, there are chances that components might fail much before yield, hence it's very important to study the components in RF from fatigue perspective. In my personal experience, I can explain fatigue to anyone who has done cycling that they must have felt this tension-compression load in their legs and if they do it for a longer duration(cycles) then their legs feel that fatigue.

Coming back to the component of my interest BC, where I experienced hotspots in the ULC in GM. The SN curve data which has fatigue strengths on Y axis and Number of cycles on X, is shown below in Figure 3 and is taken from Euro code 3.

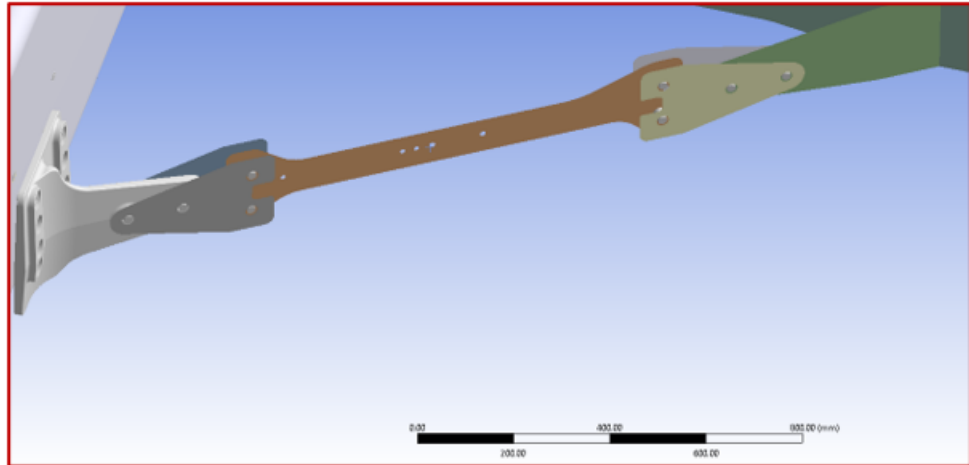


Figure 2: Geometry of Bottom cross

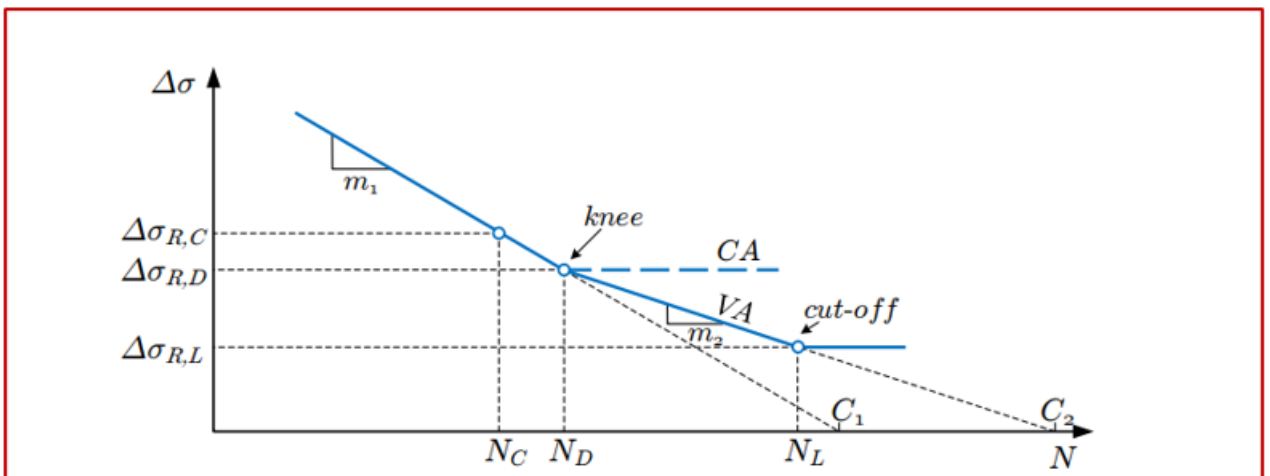


Figure 3: SN curve details

The stresses in terms of 6 tensors (3 Normal and 3 shear components) at nodes from the BC were extracted in FEA and for the maximum stress I calculated the fatigue life from the SN curve and a comparison with the number of load cycles, the data of which comes from sensors, gives me the damage value from Palmgren-Miner rule.

2.2 Flowchart of the process

The process of mitigating the fatigue hotspots starts with extraction of 6 tensors of stresses through a script, after running the ULC in FEA. The SN curve data is taken

from Eurocode 3, from the maximum stresses on all the nodes extracted, I calculate the fatigue life in terms of number of cycles. From sensor data I get the load time series, then

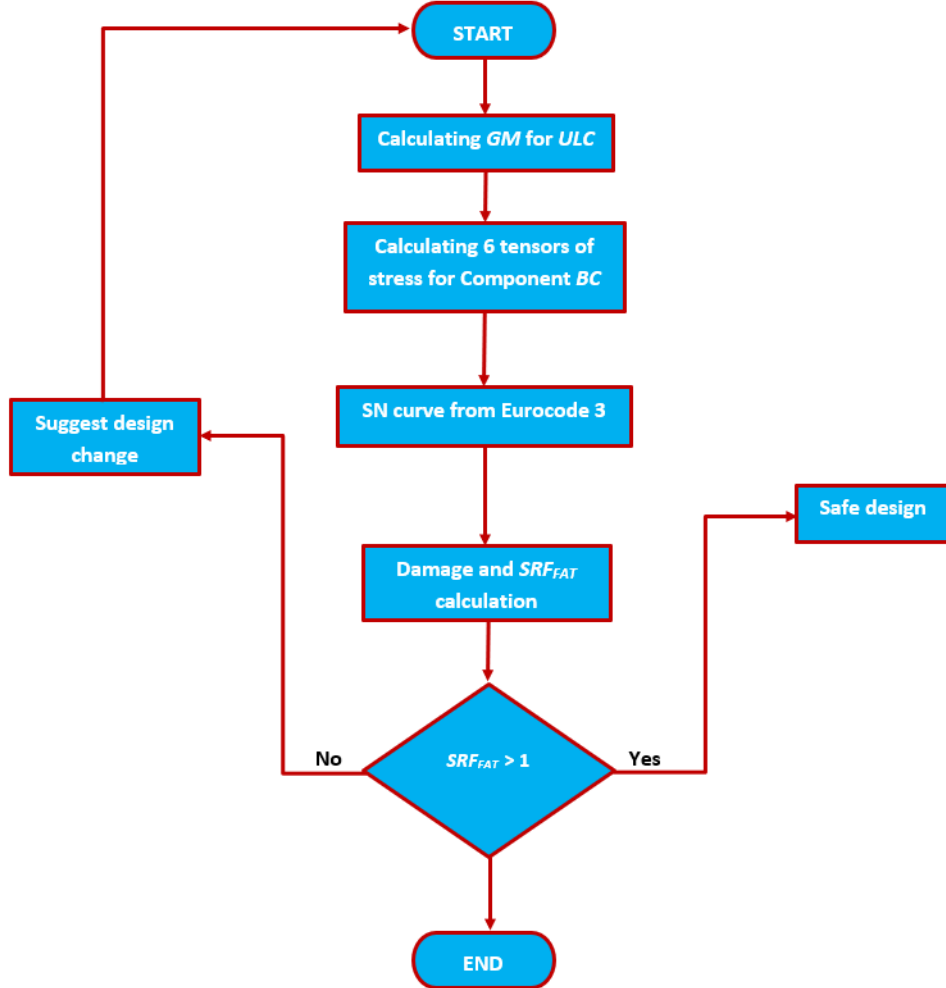


Figure 4: Fatigue mitigation process Flowchart

I take reference from Palmgren-Miner rule and compare the two to calculate fraction of life consumed by a stress cycle, this is also called as damage. Once I calculate the damage, I take inverse of it for all nodes to calculate for SRF_{FAT} (Stress reserve factor fatigue), the success criteria for the SRF_{FAT} is they must be all greater than 1, in case the SRF_{FAT} are below 1, I look for redesign and follow the same steps again, the process flowchart is shown in Figure 4 above.

2.3 Stress tensor extraction and SN curve

First of all, nodes were selected and given a named selection in FEA, for all these nodes, 6 stress tensors were extracted, 3 Normal and 3 shear stresses, the APDL script that I formulated. The SN curve data which gives the behavior of structural steel under a cyclic loading, in terms of number of cycles and fatigue strength, I take Detail Category (DC) curve from Euro-code 3.

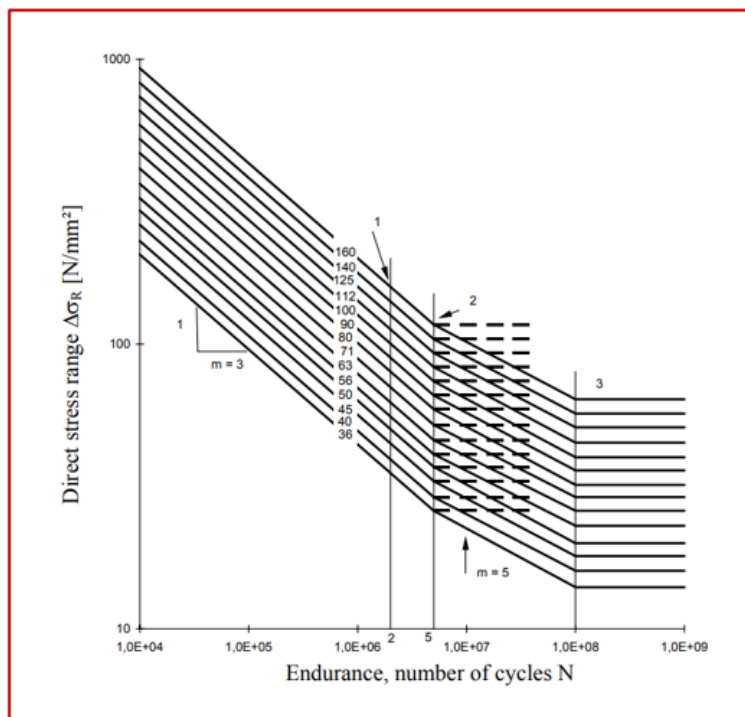


Figure 5: SN curve for different DC category

Since in the global model I saw that the hotspots were related to edges in BC, hence I took the SN curve for DC 125, this can also be seen with the SRF_{FAT} results shown

below for BC in Figure 6, this image clearly shows that hotspots originating from slot edges.

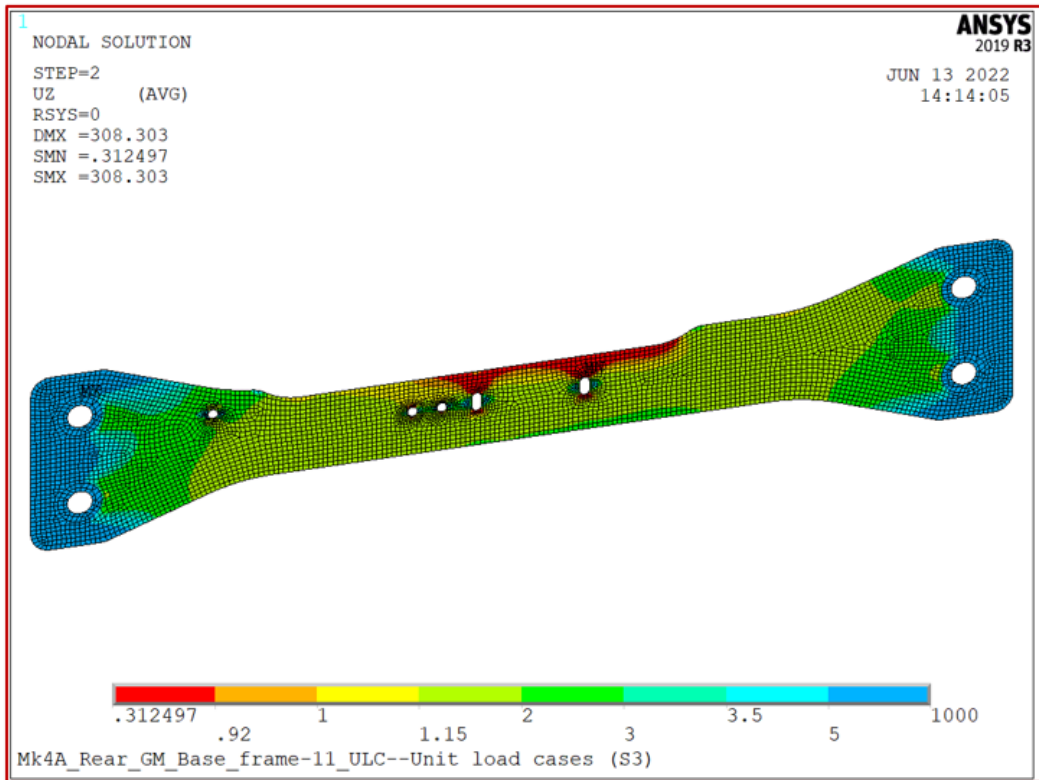


Figure 6: First iteration for Bottom cross

2.4 Relation between SN curve and Load-time series

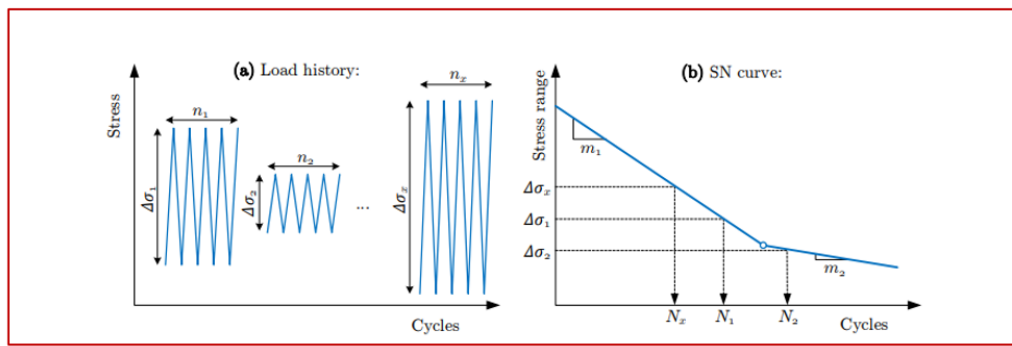


Figure 7: Load-time series and SN curve

After finalizing which SN curve data that I need to use, I needed to import the time series data from the sensor load files that I get from loads department, which they collect

from sensors installed in Wind turbine. In Figure 6, the loads operating for a certain number of cycles is shown in left side, and for each of these stresses ($\Delta\sigma_x$) fatigue life is calculated in terms of number of cycles (N_x) from SN curve, shown in right side of Figure 6.

The cumulative damage (D) is calculated through Eq.1 shown below.

$$D = \frac{n_1}{N_1} + \frac{n_2}{N_2} + \frac{n_3}{N_3} + \dots - \frac{n_x}{N_x} \quad (1)$$

Failure is assumed when the damage sum crosses 1, and I followed this as success criteria. In VESTAS, I needed to inverse this damage and found out SRF_{FAT} and it has to be above 1 for all nodes. In further sections, I will put forth the iterations performed and results for fatigue mitigation in terms of SRF_{FAT} .

2.5 Design Iterations for Bottom cross (BC)

In this section I will explain the various design iterations and how this fatigue hotspot was mitigated, from Figure 5, it can be seen that these hotspots are related to edges of the slots, so the obvious choice for me was to reduce the slot sizes in vertical direction and use oversized holes instead. First what I tried was provide some extra material towards

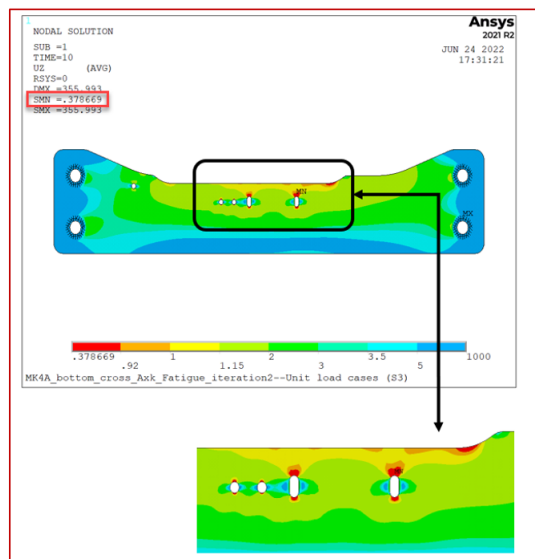


Figure 8: Second iteration for Bottom cross

the edge, and evaluate if there was any improvement, without changing the slots, this is shown in Figure 7 below. Even in this case the SRF_{FAT} was below 1 and hence not safe.

In third iteration, I removed the slots and used oversized holes and calculated again to see if the hotspots reduce, this is shown below in Figure 9.

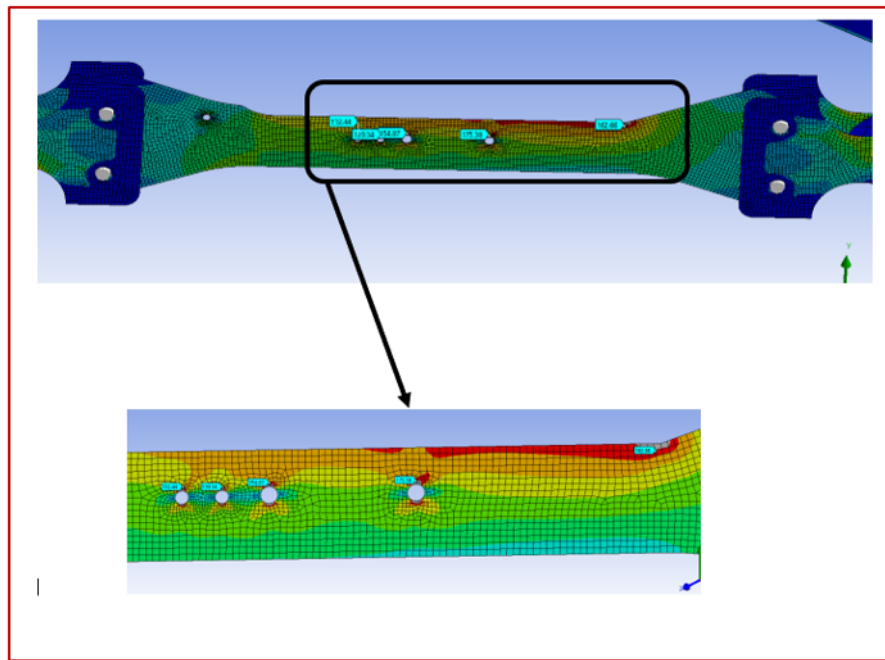


Figure 9: Third iteration for Bottom cross

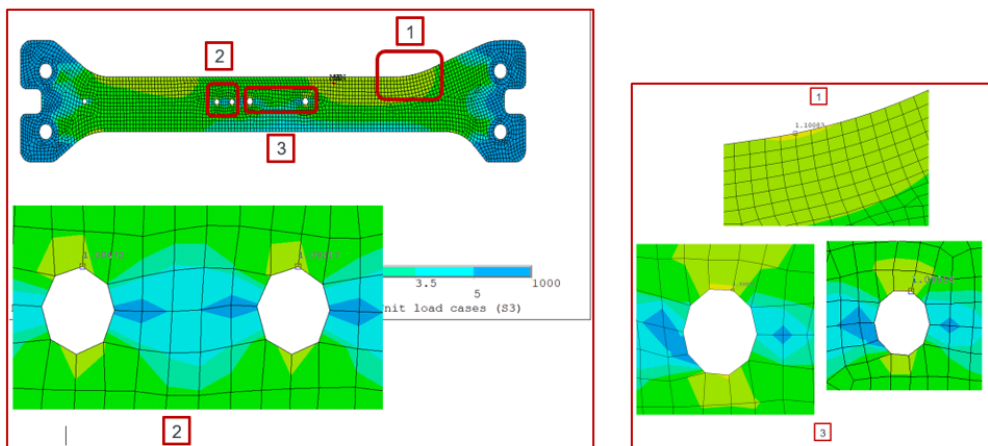


Figure 10: Fourth iteration Bottom cross

Even after 3rd iteration the fatigues hotspots were not mitigated, so in 4th iteration, I increased the plate thickness from 30mm to 40mm and re-calculated under ULC, the result for this is shown below in Figure 9, where the SRF_{FAT} are shown through probes and all SRF_{FAT} were found to be above 1.

So all the hotspots were mitigated for the Bottom cross (BC) in fatigue by redesigning the component and FEA simulation.

2.6 Summary

The fatigue mitigation project demanded skills and knowledge in the field of fatigue, in fatigue components can fail much below yield limit, and it's very difficult to detect with any pointers before the fracture happens, hence it's pertinent to have the components calculated in FEA before making the prototype.

The fatigue mitigation task involved changing the design of the BC, so as to improve the hotspots, this project was interesting in the sense that I got a chance to develop the component from scratch and do design as well as FEA.

The final results of the fatigue mitigation for BC were part of Design verification report (DVRE), I also regularly discussed with my team lead on the FEA, calculation results and DVRE, this report was used for getting certification from the DNV for the new turbine. My manager gave me this work, as I had earlier design and development experience and along-with my FEA knowledge I was able to mitigate the fatigue hotspots.

3 Project 2: Weld extrapolation for toe failure

3.1 Problem definition

This problem concerns with weld extrapolation for welded components which showed hotspots near the toe or the root of the weld in the Rear Frame (RF) of Nacelle in a Wind Turbine Generator (WTG). The Global model for the RF is shown in Figure 1 below. As can be seen the RF consists of many welded components which needs validation through FEA under various LCs.

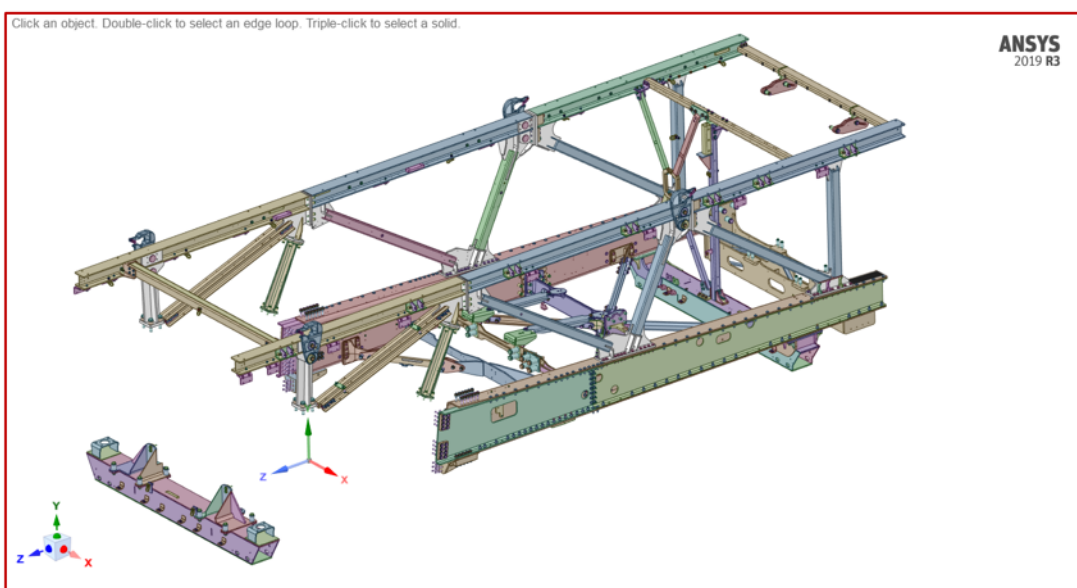


Figure 11: Global model GM

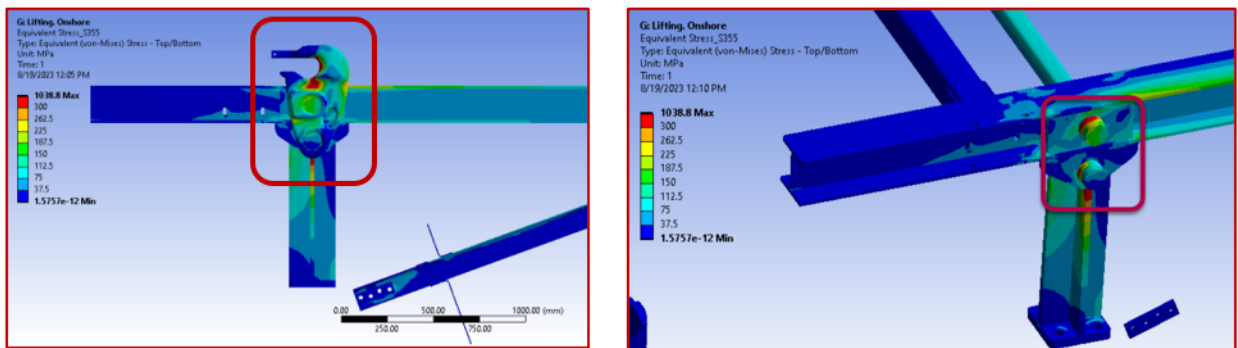


Figure 12: Detail of the hotspot around lifting pins

I work in the Finite Element Analysis (FEA) of the RF components as Lead Engineer, where I have to analyse the GM for various LCs, the LCs are mainly decided on what load would be coming to these components during operation, handling and during the service lifetime of the WTG.

Lifting scenarios (onshore and offshore), transport loads while handling, wind loads during operation, fatigue (tension-compression cycle) and other extreme LCs are simulated in FEA, these loads are applied in terms of accelerations to the RF components.

Von-Mises stress plot for the Lifting onshore LC near front hook is shown in Figure 12, details of the hotspot is also shown in Figure 12, I needed to perform this first-hand screening for all LCs, for the welds in the GM, and if I observe any hotspots then I go into more detailed study like weld extrapolation for root or toe failure check for each of these hotspots at submodel level.

I extrapolate the stresses as per Hot-spot stress method (HSS), given in IIW for toe failure check or J.D.Sørensen method for root failure check.

3.2 Flowchart of the process

The weld extrapolation task involves calculation for the GM in all LCs and then evaluating weld related hotspots in terms of stresses, once I see any hotspots in after running the GM, I would prepare a sub-model with solid plates and welds with exact representation.

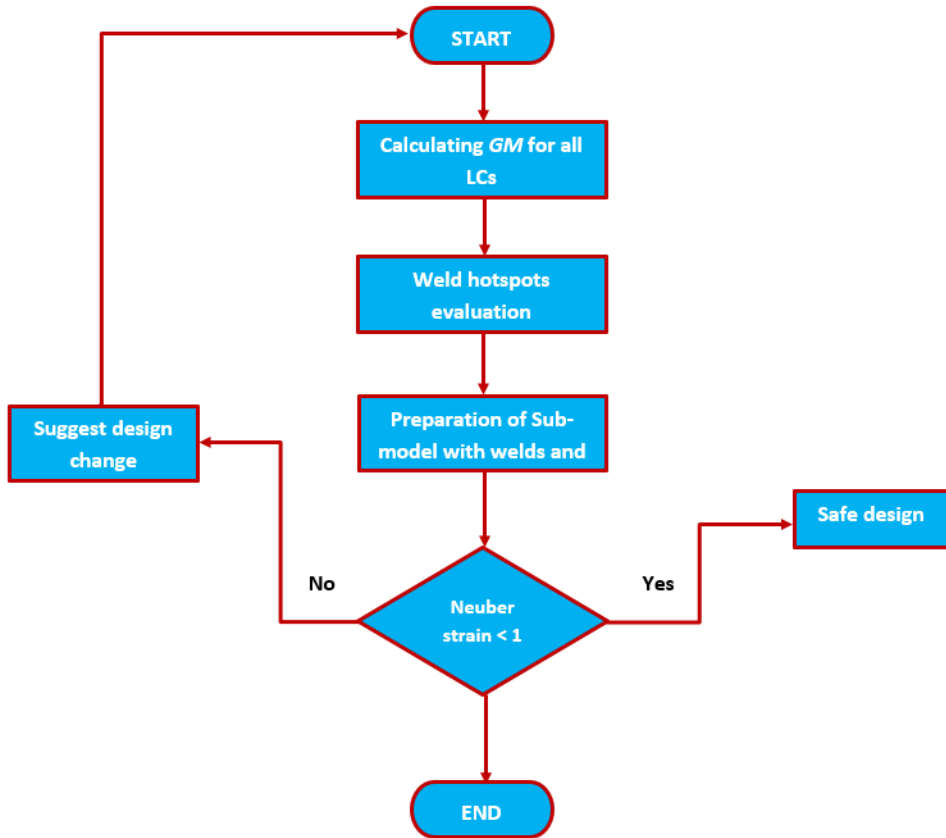


Figure 13: Weld extrapolation Process Flowchart

So, if there is a fillet weld or penetration weld the FEA model contains both, also the GM is a shell model, but the sub-model has solid plates in-order to be more accurate. A flowchart of the process followed by me is given in Figure 13.

3.3 Weld extrapolation for Toe failure

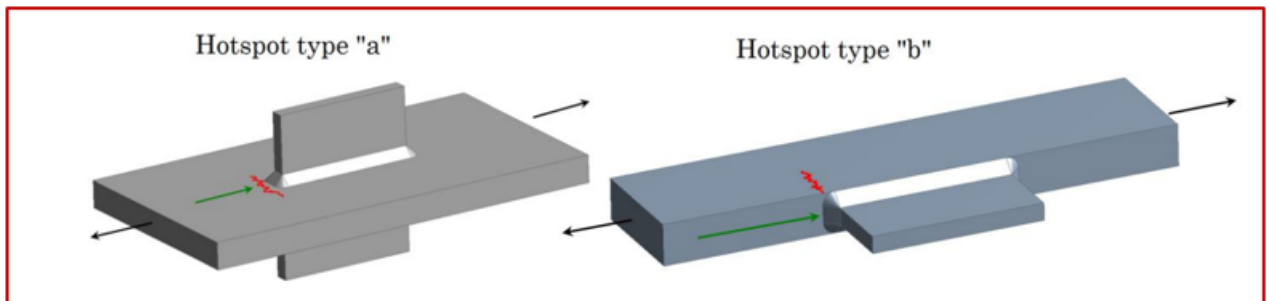


Figure 14: Type "a" and type "b" classification by IIW

Once I simulate for a particular LC, and using proper constraints in the FEA, I observe for weld related hotspots, something which is shown above in Figure 14.

I first evaluated which kind of weld failure the component can go through either toe or root failure.

The toe failure given by HSS method, the type "a" and type "b" hotspot classification comes from where is the hotspot and what kind of crack it can induce, if the hotspot can induce a crack on the weld toe it's type "a" and if the hotspot can induce the crack on the plate then it's type "b", shown in Figure 14.

The stresses calculated at weld toe can increase infinitely as I reduce the mesh size, hence it's always advisable to extrapolate stresses away from the weld. For type a extrapolation thickness of the plate comes into picture and I define two paths one at $0.4 \cdot t$ and another at $1 \cdot t$ distances from the toe of the weld, for type "b" the paths are independent of plate thickness and are defined at 4mm, 8mm and 12mm from the toe of the weld. The two extrapolation techniques are also shown below in Figure 15.

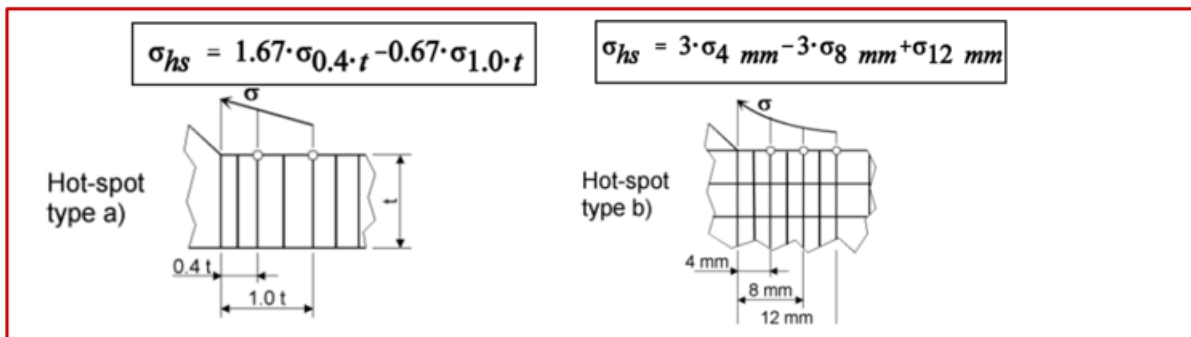


Figure 15: Type "a" and type "b" extrapolation

3.4 Weld extrapolation for root failure

The weld root failure is more common in fillet welds and I usually recommend designers to go for penetration weld where toe failure would be more common, the reason being that toe failure is easily inspectable whereas the root failure is not.

For some places in GM, where I see fillet welds and thickness of plates is not much, there I extrapolate for root failure. The method for root failure extrapolation is given by

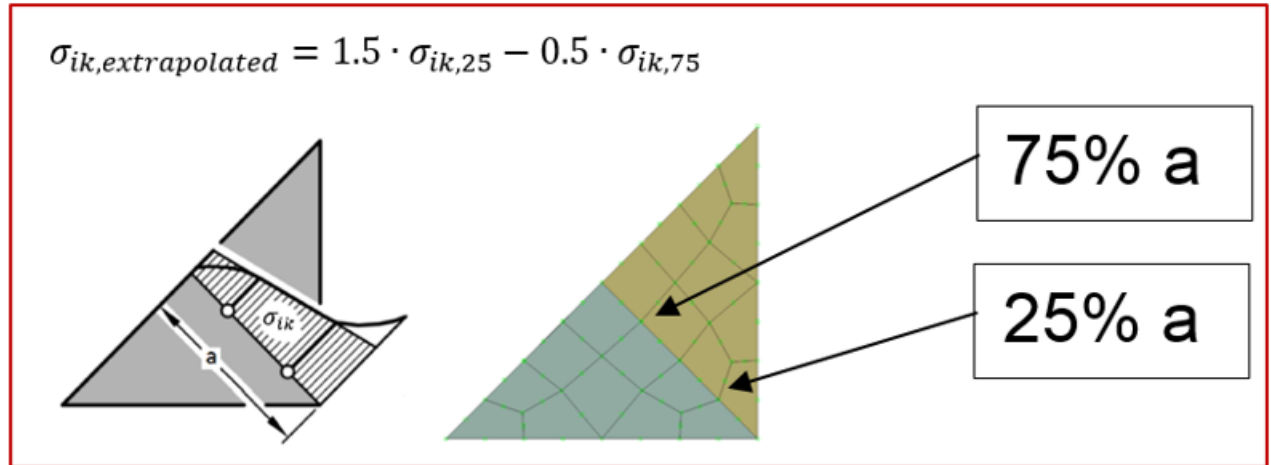


Figure 16: Extrapolation for root failure

Sørensen, J. D. and is also shown in Figure 16.

3.5 Neuber strain

Once I have the maximum principal stresses calculated along the predefined paths, I calculate the Neuber strains for the maximum extrapolated stress. Neuber strain is a linear way to calculate for strains even when components go into plasticity, it's a linear way in which I don't need to introduce material non-linearity in the FEA model, the success criterion in this case is Neuber strains < 1%.

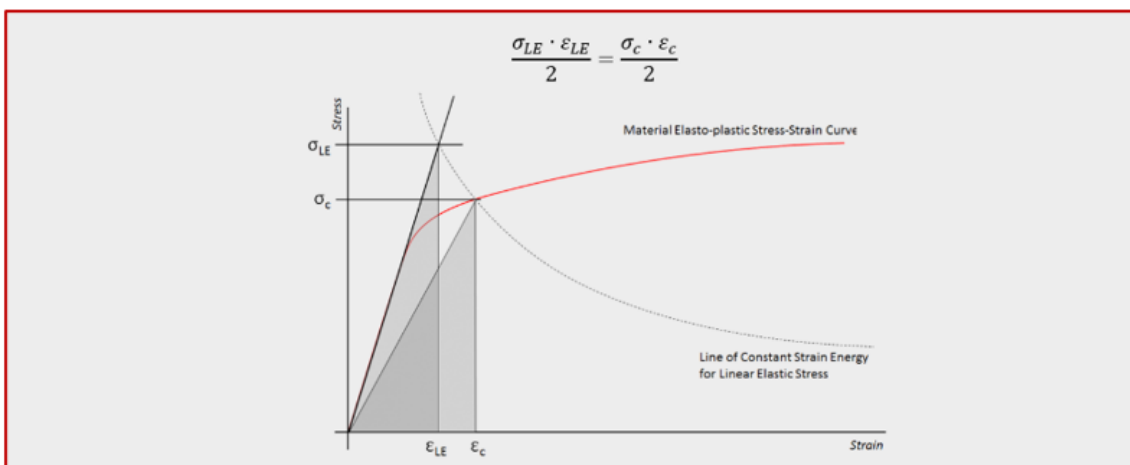


Figure 17: Neuber strain

The idea of Neuber strain is shown below in Figure 17, where strain energies in elasto-plastic and the linear case are equated.

Once I calculate the Neuber strain for maximum extrapolated stress then the strain must be below 1%, then only I consider it safe. If the strains are higher than 1% then I suggest for redesign in terms of weld sizes or changing the plates stiffness.

Below in Figure 18, the hotspot in the GM is shown which was calculated for lifting LC, once I observed the hotspot at the plate joints and pin joints, then I prepared a submodel with solid members and fillet welds, details of the fillet welds were taken from the manufacturing drawing.

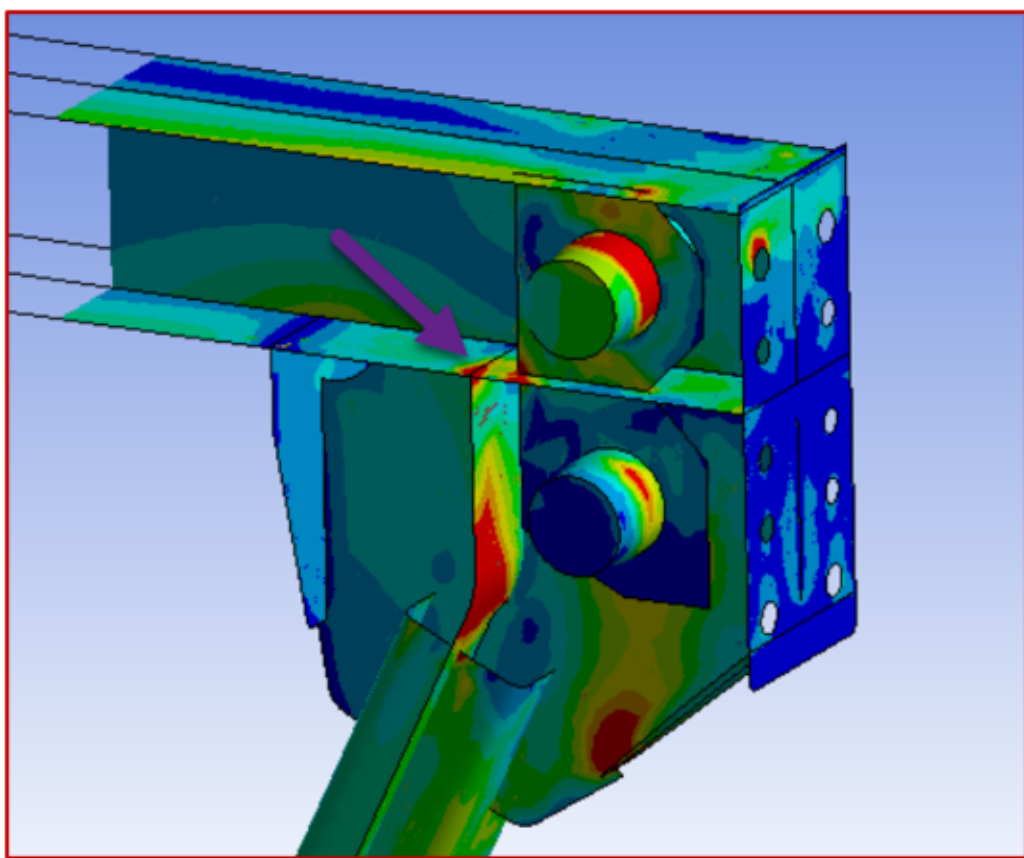


Figure 18: Weld hotspot near plates in GM

The sub-model with the actual fillet welds and solid plates is shown in Figure 19, the paths for weld stress extrapolation is shown in Figure 19 with the help of arrows, as this was type "a", hence I made splits at $0.4 \cdot t$ and $1 \cdot t$ from the toe of the weld and extrapolated for maximum principal stresses along these paths.

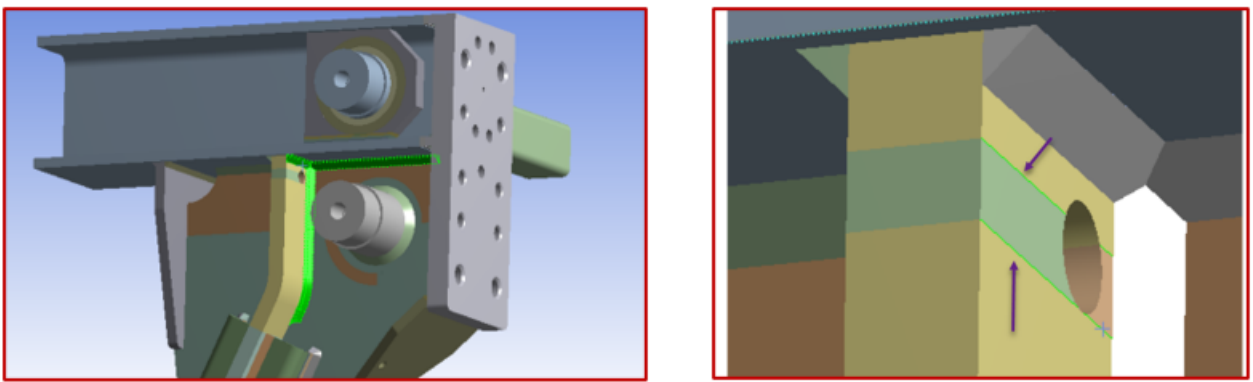


Figure 19: Fillet welds and extrapolation paths

Figure 20, below shows the extrapolation sheet where I put all the extrapolated principal stresses along $0.4 \cdot t$ and $1 \cdot t$ and calculating for Neuber strain with maximum principal stress and checking if it crosses 1% limiting value.

Elastic modulus:	210000	Yield strength:	355
Hot-spot type "a"	Hot-spot type "a"		Hot-spot type "b"
Linear extrapolation	$\sigma_{\text{hp}} = 1.67 \cdot \sigma_{0.4 \cdot t} - 0.67 \cdot \sigma_{1.0 \cdot t}$	$\sigma_{\text{hp}} = 2.52 \cdot \sigma_{0.4 \cdot t} - 2.24 \cdot \sigma_{0.9 \cdot t} + 0.72 \cdot \sigma_{1.4 \cdot t}$	$\sigma_{\text{hp}} = 3 \cdot \sigma_{4 \text{ mm}^{-3}} \cdot \sigma_8 \text{ mm}^{-1} \cdot \sigma_{12 \text{ mm}}$
	Neuber: 0.82%	Neuber: 0.00%	Neuber: 0.00%
	Max: 745.4	Max: 0.0	Max: 0.0
Length, mm	0.4t	1t	Extr
0	436.99	323.8	512.8
4.471	460.26	333.2	545.4
8.9419	483.55	342.6	578.0
13.277	505.24	352.1	604.5
17.312	522.98	361.7	631.1
21.307	539.92	371.0	653.1
25.303	556.96	380.4	675.7
29.111	569.41	389.1	696.7
33.840	581.01	397.9	716.5
36.807	591.20	406.8	734.3
40.896	600.67	415.9	752.2
44.993	607.93	425.3	764.9
49.09	615.57	435.0	743.2
53.347	617.5	428.8	764.0
57.655	619.83	432.5	765.4
61.848	617.34	434.0	729.8
66.092	615.1	435.4	723.5
70.198	611.16	436.4	728.3
74.304	607.77	437.36	722.9
78.366	598.76	434.83	708.6
82.428	590.27	432.39	690.0
86.294	578.3	425.77	680.5
90.16	566.84	419.24	665.7
94.126	554.26	411.0	650.2
98.091	542.19	403.0	635.4
102.22	525.42	394.64	613.0
106.34	509.12	386.45	591.3
110.5	490.07	374.62	567.4
114.65	488.27	363.05	558.8

Type "a" Hot spot:

The structural hot spot stress σ_{hp} is determined using the reference points and extrapolation equations as given below (see also Figure (2.2-12)).

- 1) Fine mesh with element length not larger than $0.4 \cdot t$ at the hot spot. Evaluation of nodal stresses at two reference points $0.4 \cdot t$ and $1.4 \cdot t$, and linear extrapolation (eq. 2.7)
$$\sigma_{\text{hp}} = 1.67 \cdot \sigma_{0.4 \cdot t} - 0.67 \cdot \sigma_{1.0 \cdot t} \quad (2.7)$$
- 2) Fine mesh as defined in (1) above. Evaluation of nodal stresses at three reference points $0.4 \cdot t$, $0.9 \cdot t$ and $1.4 \cdot t$, and quadratic extrapolation (eq. 2.8). This method is recommended for cross-dimensional thin layer structural areas increasing towards the hot spot, at sharp changes of direction of the applied force or for thick-walled structures.
$$\sigma_{\text{hp}} = 2.52 \cdot \sigma_{0.4 \cdot t} - 2.24 \cdot \sigma_{0.9 \cdot t} + 0.72 \cdot \sigma_{1.4 \cdot t} \quad (2.8)$$
- 3) Coarse mesh with higher order elements having lengths equal to plate thickness at the hot spot. Evaluation of nodal stresses at two reference points $0.4 \cdot t$ and $1.4 \cdot t$, and linear extrapolation (eq. 2.9)
$$\sigma_{\text{hp}} = 3 \cdot \sigma_{4 \text{ mm}^{-3}} \cdot \sigma_8 \text{ mm}^{-1} \cdot \sigma_{12 \text{ mm}} \quad (2.9)$$

Application of the mesh with the thickness increments as given in section 1.2.2 is required when the structural hot spot of type "a" is determined by surface extrapolation. For circular tubular joints, the wall thickness correction exponent of $n=0.4$ is recommended.

Fig. (2.2-10): Types of Hot Spots

$\sigma_{\text{hp}} = 1.67 \cdot \sigma_{0.4 \cdot t} - 0.67 \cdot \sigma_{1.0 \cdot t}$

$\sigma_{\text{hp}} = 3 \cdot \sigma_{4 \text{ mm}^{-3}} \cdot \sigma_8 \text{ mm}^{-1} \cdot \sigma_{12 \text{ mm}}$

Figure 20: Calculation spreadsheet

3.6 Summary

This project for weld extrapolation was given to me by my manager, who saw capability in me to solve this. Preparing the analytical spreadsheet, the GM filtering for weld hotspots, the extrapolations in FEA sub-model, was a lengthy and challenging task. To get the model close to accurate I had modelled all things as it was in real.

This work was documented in the form of a Design verification report (DVRE), which goes for certification from bodies like DNV, preparation of this report was also my task, I regularly discussed with my team lead about the FEA results and DVRE. As these tasks were something that I really enjoyed, so most of the challenges I faced were mitigated by looking through more standards.

Whenever I saw some welds were not passing, then I would talk to the designer for a possible change in the type, size of the welds and if there was any possibility for a design change in the plates itself.

4 Bolted joint verification

4.1 Problem definition

This problem concerns with bolted joints calculation for the Rear Frame of Nacelle in a Wind Turbine Generator. Nacelle structure is mainly meant to carry the gearbox, the generator, along-with other electrical components, and to mount these components you need some supporting structure.

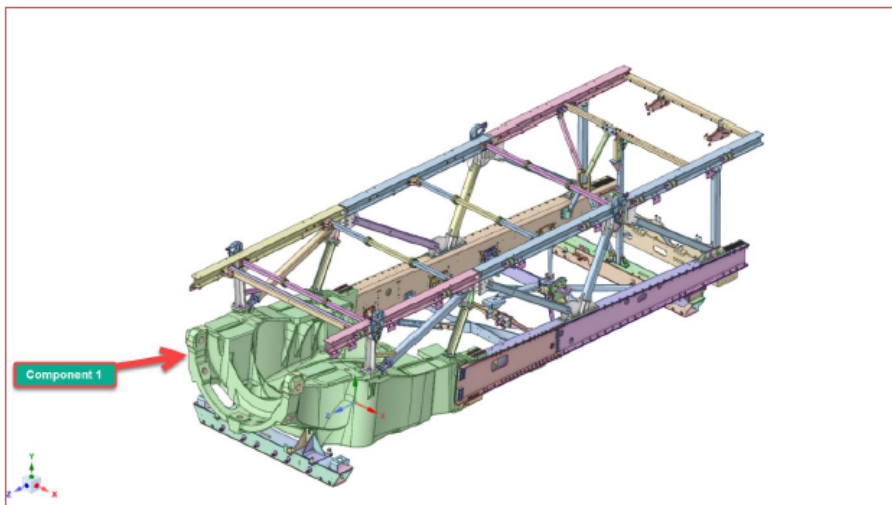


Figure 21: Nacelle RearFrame

We in WTG industry divide these supporting structures into two main categories, structure that supports gearbox is called a Base-Frame (Component 1 in Figure 21), which is mainly a casted component. To support the generator, transformer, control cabinets, towards the rear side of the nacelle, we use a structure that has welded and bolted components, we call this structure as Rear Frame (RF) Figure 22.

I work in the Finite element analysis (FEA) of the RF components as Lead Engineer, one of the first step was to reduce the solid RF model to shell and beams, in-order to reduce the size of the problem. For different Load Cases (LCs), the bolted joints were calculated for slip and tension by me.

The LCs are mainly decided on what load would be coming to these components during operation, handling and during the lifetime of the WTG. Lifting scenarios (onshore and

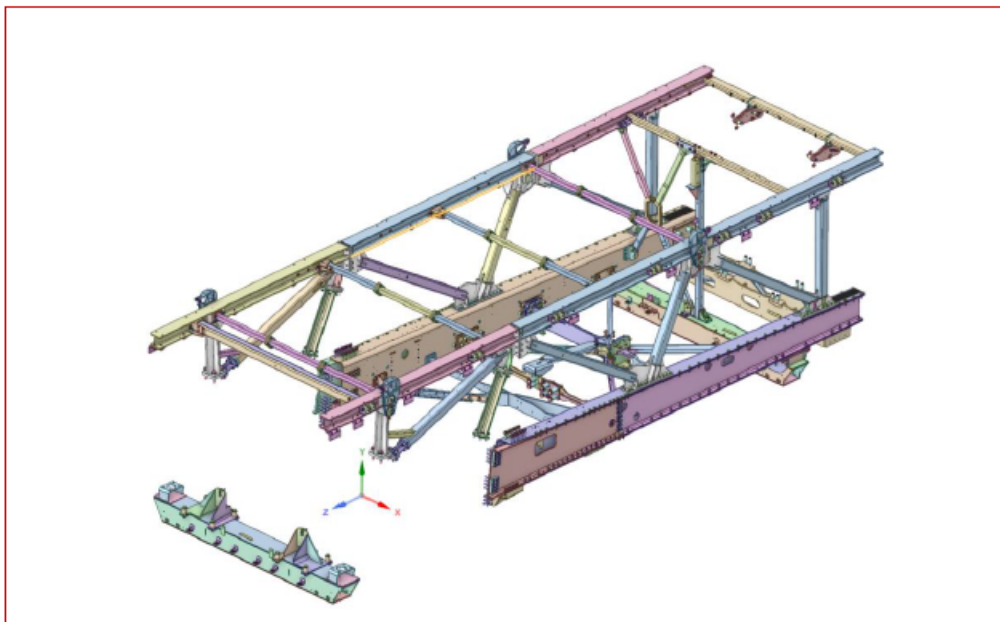


Figure 22: Nacelle RearFrame

offshore), transport loads while handling, wind loads during operation, and other extreme LCs are simulated in FEA, these loads are applied in terms of accelerations to the RF components.

4.2 Flowchart of the process

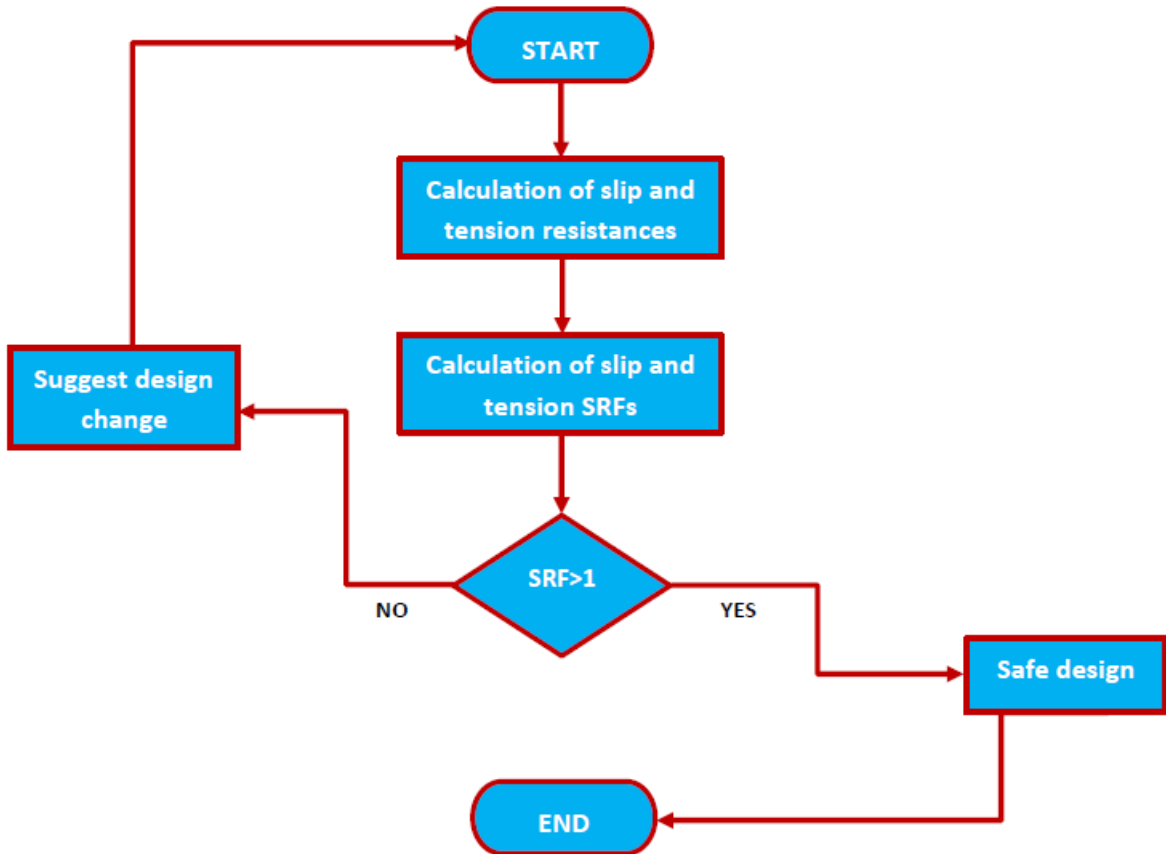


Figure 23: Process Flowchart

The bolt verification task involves calculation for shear and axial forces in the bolts modelled as beams in the FEA, from different LC, then taking these forces and analytically calculating for the slip and tension resistance check for all these bolts in RF. The resistances were made non-dimensional by comparing them with the tension and shear forces and that parameter we call as Safety reserve factor (SRF). A flowchart of the process followed is given in Figure 23.

4.3 Beam force extraction

Once we simulate for a particular LC, and using proper constraints in the FEA, we can extract the forces through beam probe or scripts. The extraction gives us the shear and axial forces which are starting points for our calculation. Figure 24 shows the position for one such beam force extraction, and Figure 25 shows the axial and shear forces extracted.

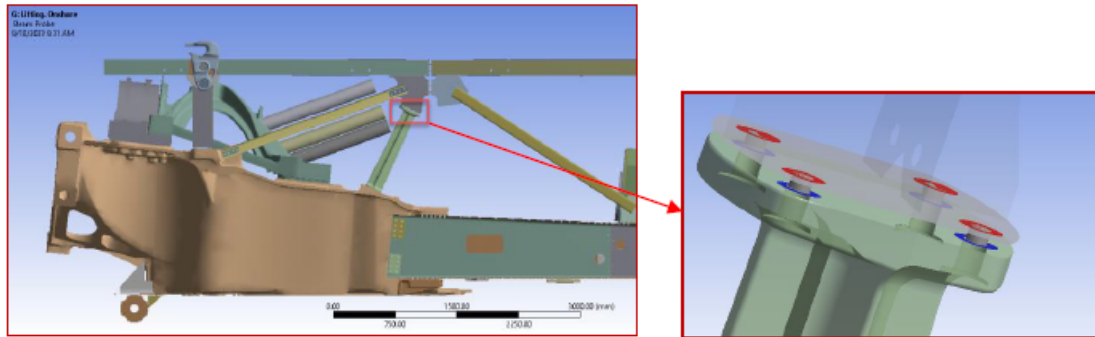


Figure 24: Beam connection shown

Definition	
Type	Beam Probe
Boundary Condition	G1010101.3(Rear frame)
Suppressed	No
Options	
Result Selection	All
<input type="checkbox"/> Display Time	End Time
Results	
Maximum Value Over Time	
<input type="checkbox"/> Axial Force	28836 N
<input type="checkbox"/> Torque	-28343 N·mm
<input type="checkbox"/> Shear Force At I	8487.7 N
<input type="checkbox"/> Shear Force At J	8487.7 N
<input type="checkbox"/> Moment At I	7.4826e+005 N·mm
<input type="checkbox"/> Moment At J	7.1255e+005 N·mm

Figure 25: Axial and shear force from Beam

4.4 Calculation of the Joint stiffness factor/Load factor Φ

After I got the forces, the next important parameter was Load factor (Φ), which speaks about the portion of total axial force coming to the bolts during the operation.

So, once I know this share, I could move to the next step of reducing the clamping force by this magnitude of force coming to the plates in order to understand the remaining clamp force, this is also shown below in Eq. 2.

$$\Phi = \frac{F_{SA}}{F_A} \quad (2)$$

Where,

F_{SA} is the force coming to the Bolt

F_A is the axial force on the joint (From beam force extraction)

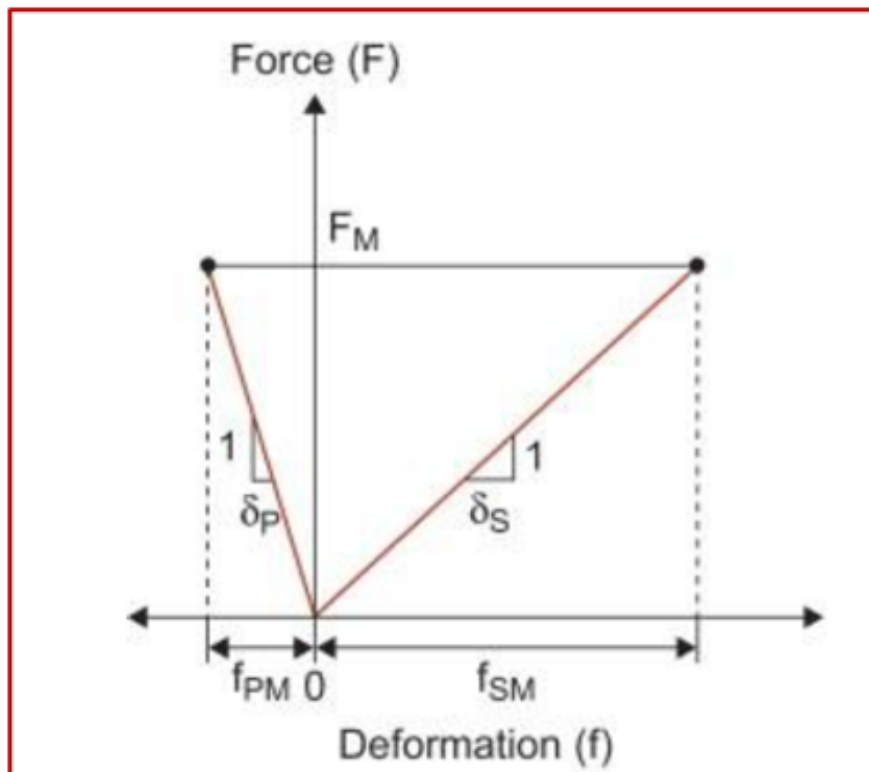


Figure 26: Bolt joint loading diagram under preload

The joint loading diagram (Figure 27) comes from VDI 2230 part 1, it gives the blueprint for the calculation and understanding of how joints behave when in assembly. In this diagram, Force Vs Deformation graph is plotted, FM is the preload on the members and drawn in absence of an axial force.

The left portion of this graph talks about plate which would be under compression, and the right side talks about the bolts under tensile loading. The positive deformation for the bolts (f_{SM}) and negative deformation for the plates (f_{PM}) are represented in this diagram.

Figure 28 shows the joint diagram of members under axial tensile load (F_A) coming to the assembly.

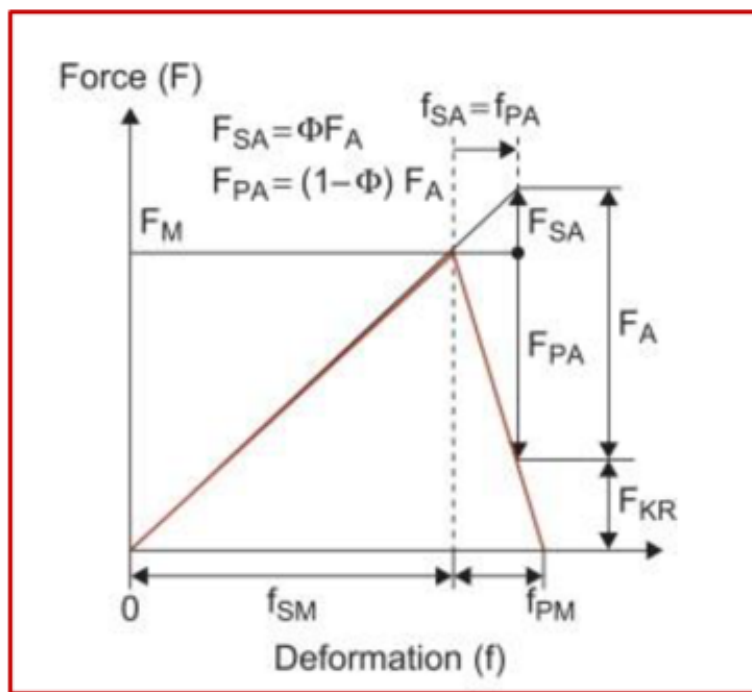


Figure 27: Bolt joint diagram under axial load

This load is shared by the bolts and the plates and mathematically can be written as:

$$F_A = F_{SA} + F_{PA} \quad (3)$$

$$\Phi = \frac{F_{SA}}{F_A} = \frac{K_b}{(K_b + K_m)} \quad (4)$$

Where,

K_b is the stiffness of the bolts

K_m is the stiffness of the member (plates)

The bolt stiffness would come from it's tensile stress area, it's nominal diameter and it's length, calculation of which is quite similar to that of a spring in tension.

On the other hand, for the members (plates), the stiffness is calculated in an integral sense, as clamp area keep on changing from the bolt head to the nut, this clamping area is in the form of a truncated cone, shown in Figure 29 below.

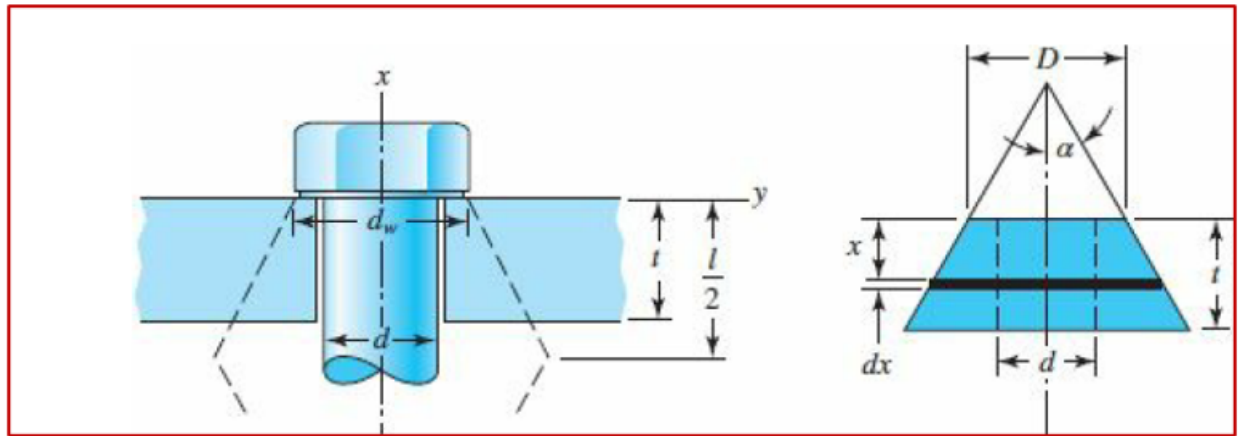


Figure 28: Pressure cone

$$F_{pc} = F_A [F_p - (1 - \Phi)] \quad (5)$$

Once I got hold of the Load factor Φ , then my focus goes to the load coming to the members (plates). As I am now aware that the Load factor Φ , is the share of axial load coming to bolts, I calculated for the force coming to the members as this tensile force would decompress and, in a sense, relieve the clamping done initially on the members. Below in Eq.6 the residual clamp force in the members is shown.

For any sliding to happen, static friction must be overcome. Figure 29 shows the general physics for two plates with the residual clamp force and static friction force.

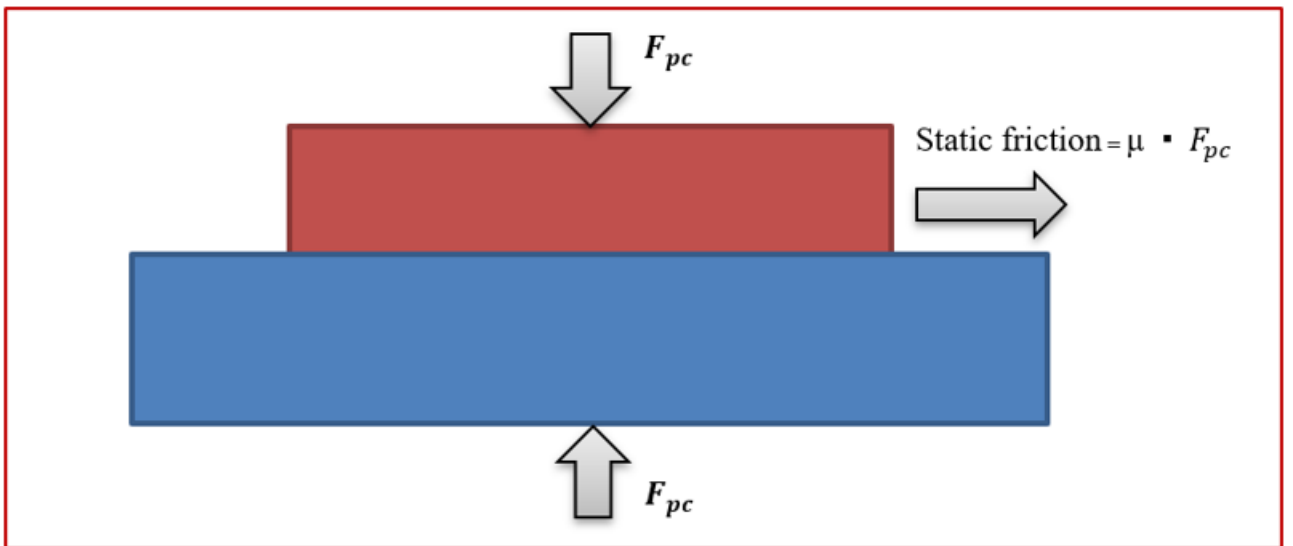


Figure 29: Static sliding between two plates

Once I calculated the limiting slip load, I include few factors such as slip resistance factor (K_s) and factor of safety to arrive at the Design Slip Resistance ($F_{S,Rd}$).

Design slip resistance ($F_{S,Rd}$) is calculated as follows:

$$F_{S,Rd} = K_s n \mu \left[\frac{F_p - (1 - \Phi) F_A}{\gamma_{M3}} \right] \quad (6)$$

Where,

K_s is the slip resistance factor, dependent on the hole shape (slotted, normal)

Partial safety factor, slip resistance at ultimate state, $\gamma_{M3} = 1.25$

Comparison is made with the shear force $F_{v,Ed}$ coming to the joints, and in order to have the joints to function properly, the shear force should always be less than the slip resistance.

$Slip_{SRF}$ and success criterion:

$$Slip_{SRF} = \frac{F_{s,Rd}}{F_{v,Ed}} > 1 \quad (7)$$

4.5 Tension resistance calculation

Bolts get stretched under the preload, then if the axial tensile force comes to the bolt then it adds up the stresses in the bolt, in-order that the bolts function safely under this acting load, I needed to first understand what is bolt's tension resistance from it's material properties (ultimate strength, f_{ub}) and cross sectional parameters (tensile stress area, A_s).

The bolt's tension resistance $F_{t,Rd}$ is calculated as:

$$F_{t,Rd} = \frac{k_2 \cdot f_{ub} \cdot A_s}{\gamma_{M2}} \quad (8)$$

Where,

A_s is tensile stress area of the Bolt

f_{ub} is the ultimate strength of the bolt, for 10.9 bolt, $f_{ub} = 1000$ MPa

Partial safety factor, resistance of the bolts, $\gamma_{M2} = 1.25$

$K_2 = 0.63$ for countersunk bolts

$K_2 = 0.90$ otherwise

The total axial load coming to the bolt is calculated as

$$F_{t,Ed} = F_p + \Phi \cdot F_A \quad (9)$$

Where,

F_p is the preload applied on the bolt

F_A is the axial force coming to the overall assembly

Φ is the load factor

Tension SRF and success criterion:

$$SRF_{Tension} = \frac{F_{t,Rd}}{F_{t,Ed}} > 1 \quad (10)$$

Again comparing the tensile force coming to the bolt (Eq.9), with the tension resistance (Eq.8), I calculated for $SRF_{Tension}$ with Eq.10.

4.6 Summary

The project demanded skills and knowledge from both the numerical FEA and analytical domains. As this was an individual project, at first I had to prepare a spreadsheet with all these formulas for tension and slip checks.

The bolt checks helped me in preparing the Design verification reports (DVRE) for the bolts in the WTG assembly, these were used to attain certification from DNV, this played a crucial role in certification of the Nacelle and overall wind turbine.

As I already had good exposure to bolt calculation with the VDI 2230 and Euro-code 3, it was an obvious choice for my manager to give me this responsibility, I also regularly discussed with my team lead on the FEA, calculation results and DVRE. With my work these bolts were evaluated and played a crucial role in the overall wind turbine certification and deployment.

5 Buckling analysis

5.1 Problem definition

As the rear frame is operation under various extreme loads, there are always chances of channels to buckle under compressive and bending loads.

This has to be checked by extracting forces in the beams in normal direction. The exact steps are mentioned in the subsequent subsection.

5.2 Design Buckling resistance, $\alpha_{b,Rd}$

Step 1

- Load multiplier check

The first step is to check the load multiplier from the Eigen-Value Buckling analysis of the assembly.

BS EN 1993-1-1:2005
EN 1993-1-1:2005 (E)

5.2 Global analysis

5.2.1 Effects of deformed geometry of the structure

- (1) The internal forces and moments may generally be determined using either:
 - first-order analysis, using the initial geometry of the structure or
 - second-order analysis, taking into account the influence of the deformation of the structure.
- (2) The effects of the deformed geometry (second-order effects) should be considered if they increase the action effects significantly or modify significantly the structural behaviour.
- (3) First order analysis may be used for the structure, if the increase of the relevant internal forces or moments or any other change of structural behaviour caused by deformations can be neglected. This condition may be assumed to be fulfilled, if the following criterion is satisfied:

$$\begin{aligned} \alpha_{cr} &= \frac{F_{cr}}{F_{Ed}} \geq 10 && \text{for elastic analysis} \\ \alpha_{cr} &= \frac{F_{cr}}{F_{Ed}} \geq 15 && \text{for plastic analysis} \end{aligned} \quad (5.1)$$

where α_{cr} is the factor by which the design loading would have to be increased to cause elastic instability in a global mode

F_{Ed} is the design loading on the structure

F_{cr} is the elastic critical buckling load for global instability mode based on initial elastic stiffnesses

NOTE A greater limit for α_{cr} for plastic analysis is given in equation (5.1) because structural behaviour may be significantly influenced by non linear material properties in the ultimate limit state (e.g. where a frame forms plastic hinges with moment redistributions or where significant non linear deformations from semi-rigid joints occur). Where substantiated by more accurate approaches the National Annex may give a lower limit for α_{cr} for certain types of frames.

Figure 30: Load Multiplier from EC-3

This is done in pre-stressed state of any particular extreme load case. As per EN 1993-1-5:2005, the critical load should be over and above 10 times from the applied load, in the elastic analysis, this is also shown in Figure 30.

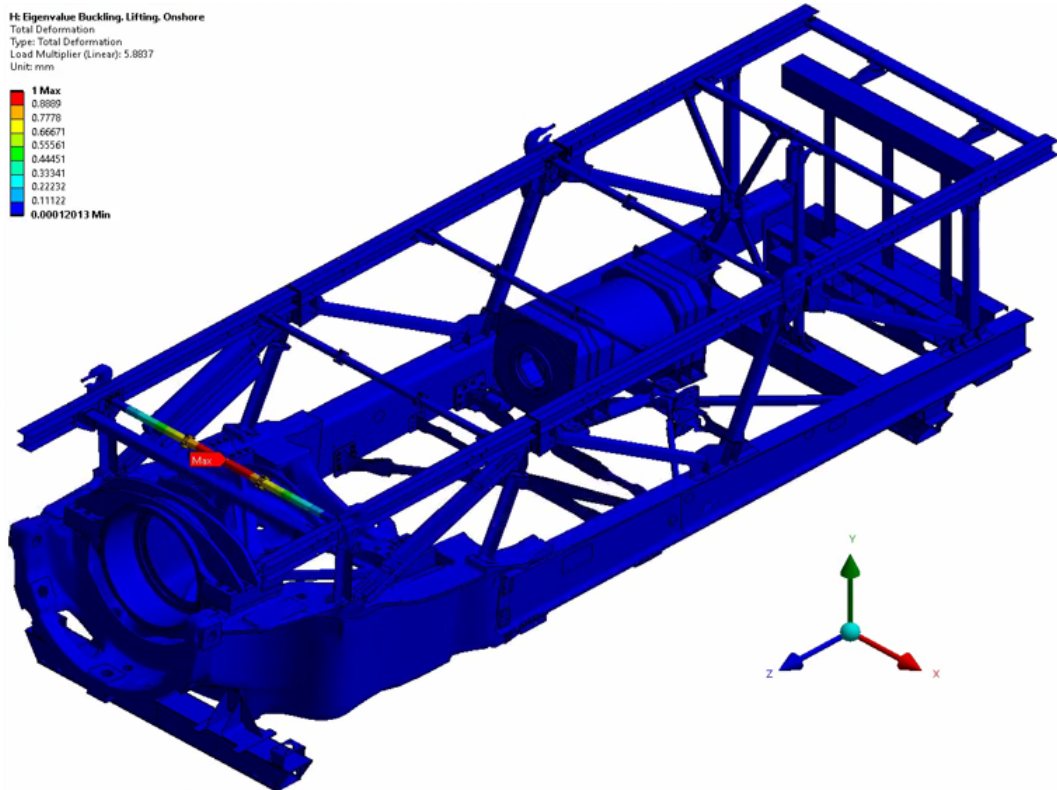


Figure 31: Load Multiplier Eigen-Value Buckling

In the Eigen-Value Buckling pre-stressed state if I observe load multiplier less than 10 (Figure 31), then I need to validate this structure either through analytical calculations or through re-design.

Step 2

- Compression load and section properties

In this part once I observe that load multiplier is less than 10, then I calculate through analytical formulas given in EN 1993-1-5 : 2005 for Design Buckling resistance (α).

In this regard first I extract the compression force coming on the channel in FEA tool, shown in Figure 32.

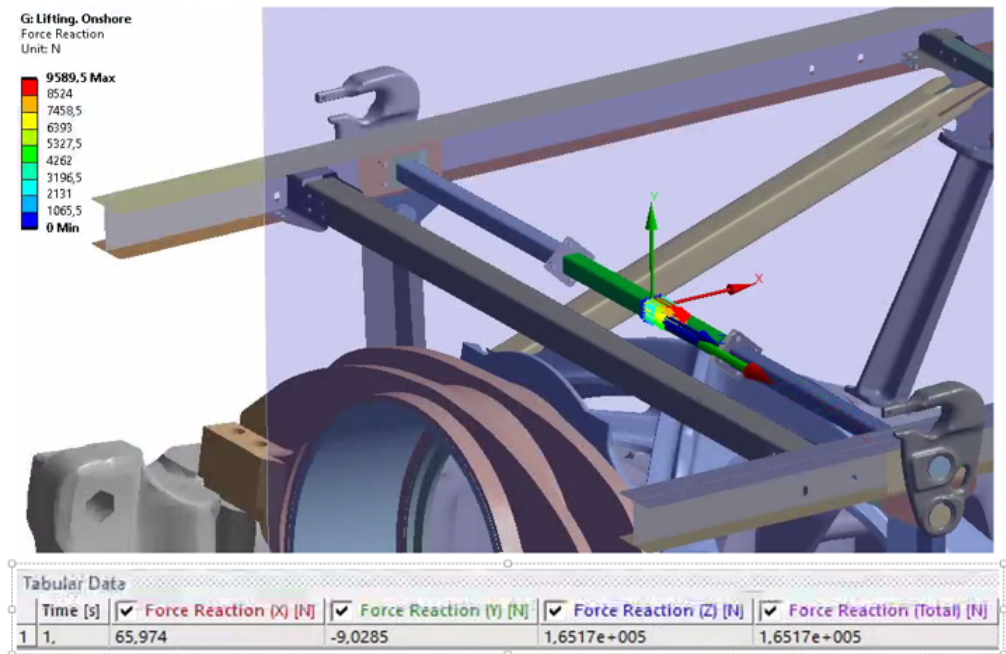


Figure 32: Max compression force on channel/Beam

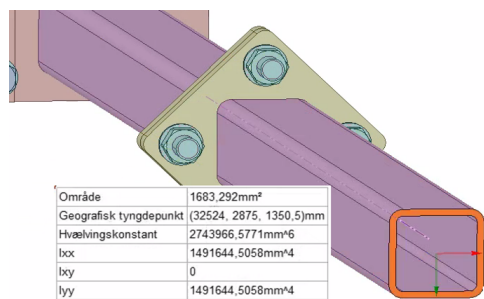


Figure 33: Moment of inertia

I also take the moment of inertia for this channel from SpaceClaim (Figure 33)

Step 3

- Slenderness ration(λ)

$$\lambda = \sqrt{\frac{Af_y}{F_{cr}}}$$

Where,

f_y = Yield limit

$$F_{cr} = \frac{\pi^2 EI}{l_e^2}$$

Step 4

- Calculation of parameter ϕ

$$\phi = 0.5[1 + \alpha(\lambda - 0.2) + \lambda^2]$$

Where,

α = is the imperfection factor and depends on Buckling curves

Buckling curve*	a_0	a	b	c	d
Imperfection factor	0.13	0.21	0.34	0.49	0.76

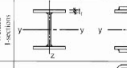
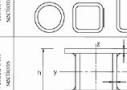
Table 6.2: Selection of buckling curve for a cross-section						
Cross section	Limits	Buckling about axis			Buckling curve	
		S 275	S 355	S 400	S 420	
Rolling sections						
	$t_u > 12$	$t_l \leq 40$ mm	$y-y$	$z-z$	b	a_b
		$40 \text{ mm} < t_l \leq 100$	$y-y$	$z-z$	b	a
		$t_l \leq 100$ mm	$y-y$	$z-z$	c	a
		$t_l > 100$ mm	$y-y$	$z-z$	d	c
Welded Sections						
	$t_l \leq 40$ mm	$y-y$	$z-z$	b	b	c
	$t_l > 40$ mm	$y-y$	$z-z$	c	c	d
Hollow Sections						
	hot finished	any	a	a_b		
	cold formed	any	c	c		
Welded box Sections						
	generally (except as below)	any	b	b		
	thick welds ($\alpha > 0.5t$) $b/t_w < 10$ $b/t_w < 50$	any	c	c		
U, T and solid Sections						
	any	c	c			

Figure 34: Buckling Curves

Step 5

- Reduction factor (χ)

$$\chi = \frac{1}{\phi + \sqrt{\phi^2 - \lambda^2}}$$

Step 6

- Design Buckling factor, $\alpha_{b,Rd}$

$$\alpha_{b,Rd} = \frac{\chi A f_y}{F_{ed}}$$

Where,

F_{ed} = Max compression force coming from FEA

Step 7

- Design Buckling factor, $\alpha_{b,Rd}$

$$\alpha_{b,Rd} = \frac{\chi A f_y}{F_{ed}}$$

If,

$\alpha_{b,Rd} > 1$, design accepted

$\alpha_{b,Rd} < 1$, design not-accepted. Non-linear analysis needs to be performed

6 Fracture mechanics

6.1 Problem definition

In fracture mechanics I have solved one problem given in a paper "Predicting extended service Life durability and damage tolerance" by David R. Dearth. The geometry of the problem is shown below in Figure 35.

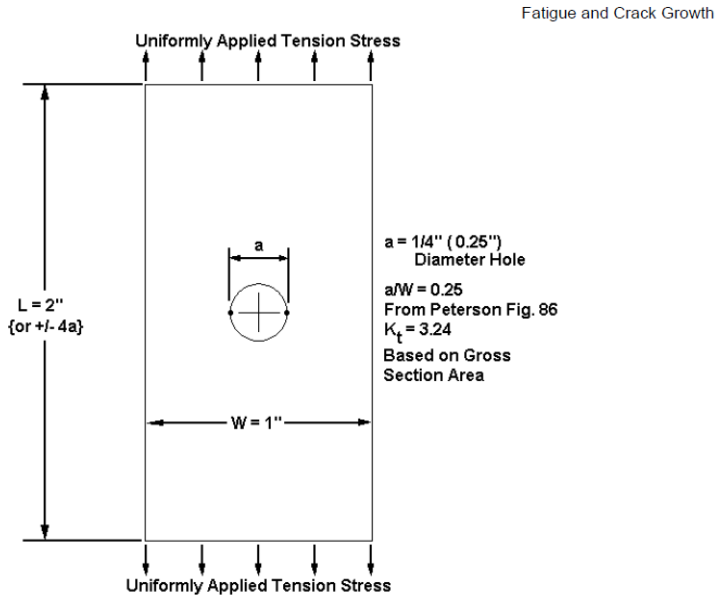


Figure 35: Geometry of plate with hole

In this geometry and loading a stress concentration factor(SCF) K_t effect is created near the edge of the hole. The plate is fabricated from aluminum alloy 2024-T4 extruded plate and is subjected to constant amplitude cyclic loading of 0 psi Minimum, to 12,000 psi Maximum.

6.2 Calculation of SCF K_t

The theoretical value can be seen from Petersons work on stress concentration factor. With the same geometric dimensions and loads I simulated to see the stress concentration factor(K_t) in FEA calculation.

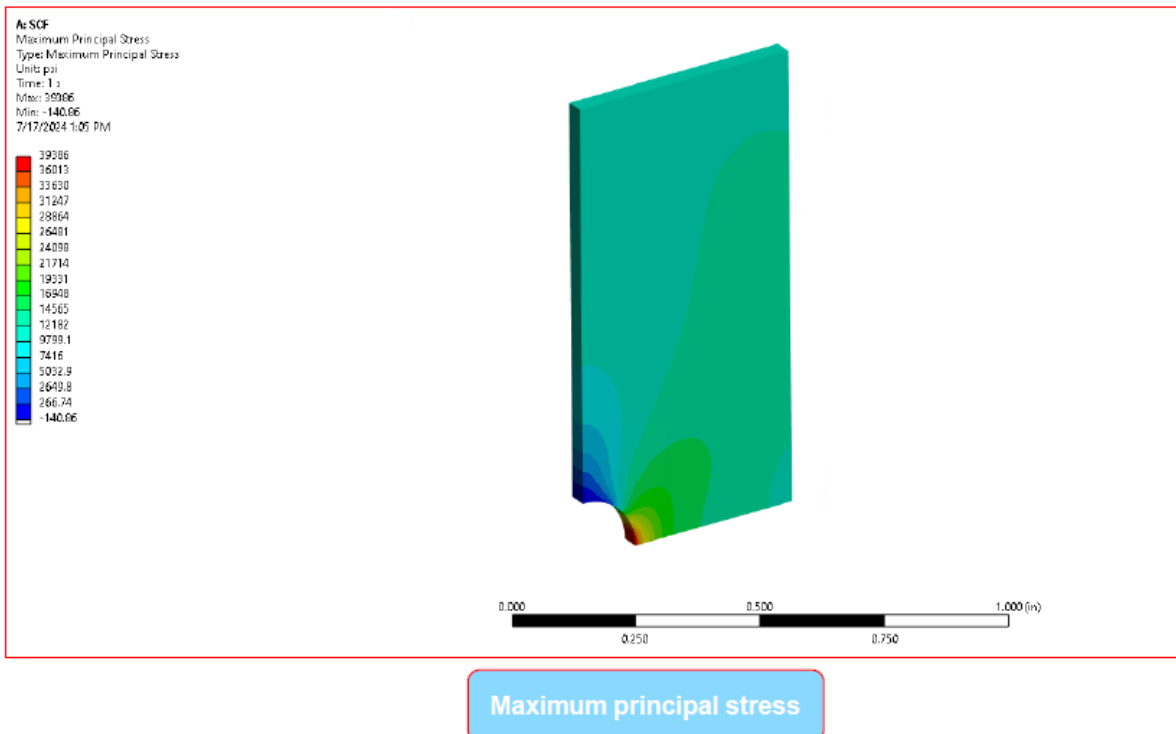


Figure 36: Maximum principal stress

Taking the ratios of the maximum principal stress and the load applied.

$$K_t = \frac{39386}{12000} = 3.28$$

Stress concentration factor Kt as per R.E. Peterson = 3.24
 So, the percentage deviation from theory to FEA is

$$\frac{3.28}{3.24} - 1 = 1.2\%$$

6.3 Fracture toughness and fatigue tool

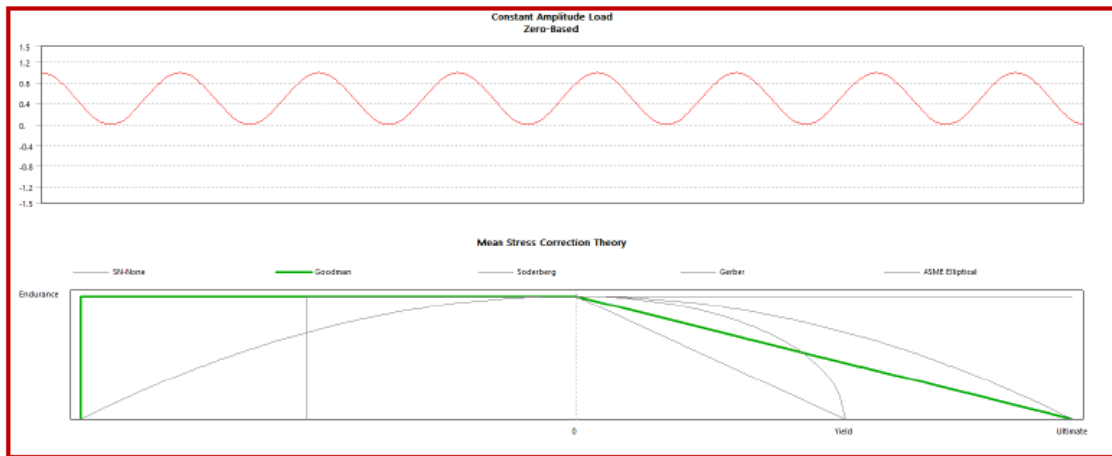


Figure 37: Goodman mean stress correction

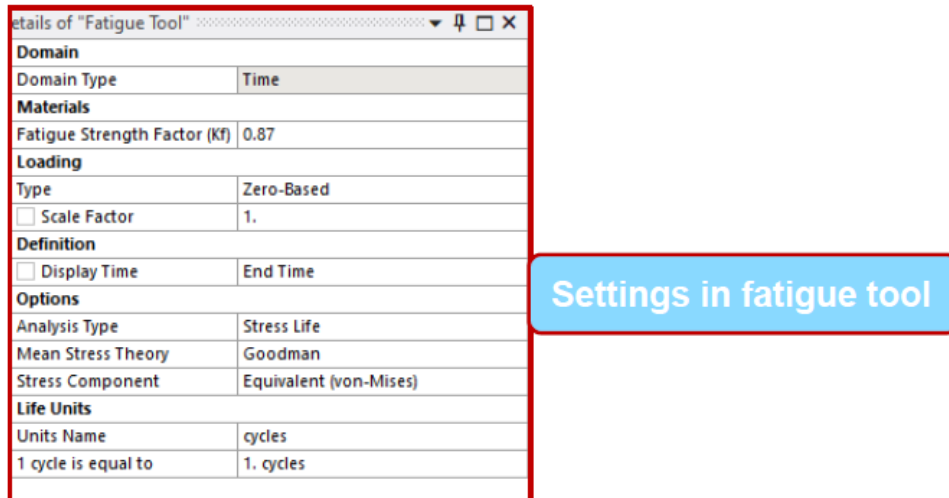
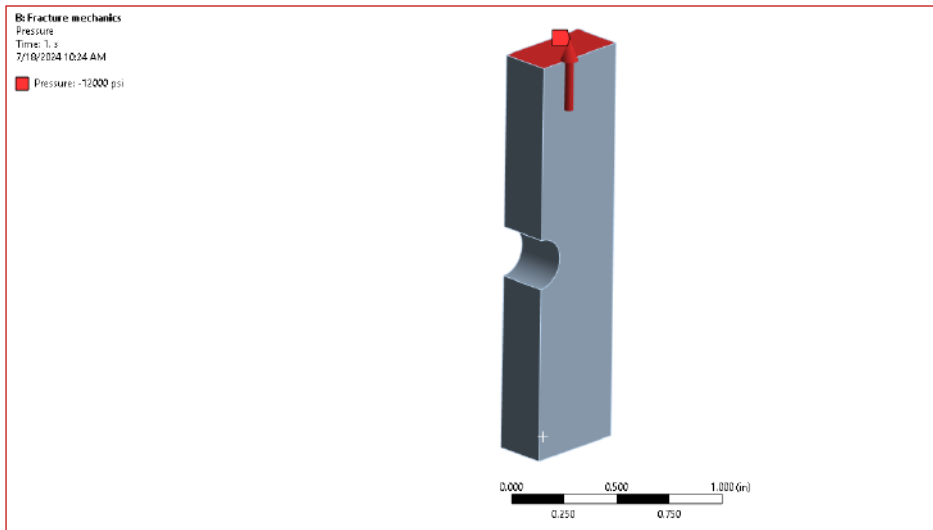


Figure 38: Fatigue tool settings

With the goodman mean stress correctin and the settings for he fatigue tool, where the load is zero-max-zero(zero based) and the analysis type is stress-based , the fatigue strength of 0.87 was taken from the paper by David R. Dearth.



Tension load (mode 1) = 12000 psi

Figure 39: Tensile loading: Mode I

I modeled an elliptical crack through the samart rack tool in ansys and calculated for the stress intensity factor mode 1 as that is the dominant mode, this is also shown in Figure 40 below.

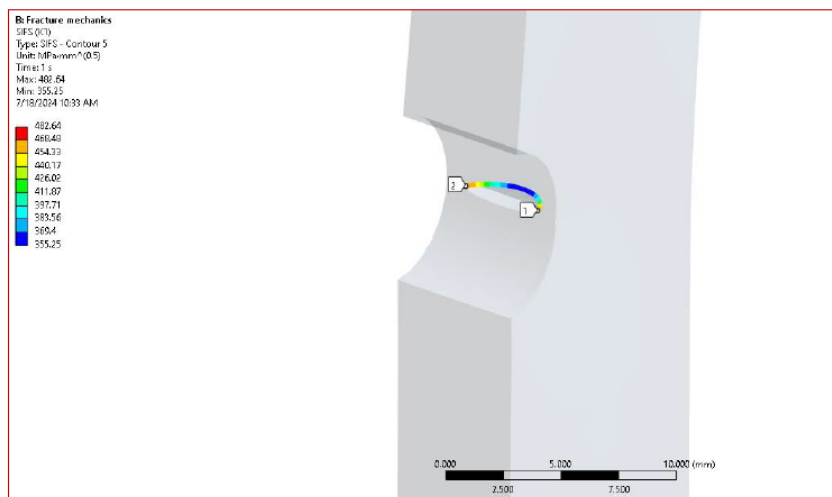


Figure 40: Elliptical crack

Definition	
Type	SIFS
Subtype	K1
Active Contour	5
Location Method	Crack Length Percentage
Crack Length Percentage	50
Suppressed	No
Options	
<input type="checkbox"/> Display Time	End Time
Spatial Resolution	Use Maximum
Results	
<input type="checkbox"/> SIFS (K1)	10225 psi.in ^{0.5}
<input type="checkbox"/> Minimum Value Over Time	8491.9 psi.in ^{0.5}
<input checked="" type="checkbox"/> Maximum Value Over Time	10225 psi.in ^{0.5}

Figure 41: Stress intensity factor K_I

The fracture toughness of the material(K_{IC}) was $30000 \text{ psi.in}^{0.5}$

The stress intensity factor in dominant mode $< K_{IC}$

7 FSI experiment of Thermal power plant chimney

7.1 Problem definition/Objective

The project was about the new construction of an industrial thermal power plant chimney, and finding certain structural parameters in extreme wind-loaded conditions and other nearby structures mimicking the thermal power plant construction in a Göttinger-Type Wind Tunnel. The structural parameters that were to be found out through experiment are mentioned below:

- Bending moment and shear force calculation for the scaled-down chimney
- Natural frequencies and damping ratios calculations through experiment
- Finding out the worst case scenario and comparison with standards IS 4998 Part 1 and IS 875 Part 3

7.2 Methodology

The experiments were conducted in a closed circuit wind tunnel with test section dimensions of $9.6\text{m} \times 1.6\text{m} \times 1.6\text{m}$, the details of the tunnel can be seen in Figure 42. In the Figure you can see that there are roughness elements and spires in front of the test section to increase the thickness of the boundary layer to 1m and in a way simulating the atmospheric boundary layer which is around 300m, hence all the components in the wind tunnel were made on 1:250 scale keeping this in mind.

The Flue-Gas Desulfurization chimney is of 150m tall and is scaled to 0.6m for experiments and similar all other nearby structures too were scaled in similar proportion.

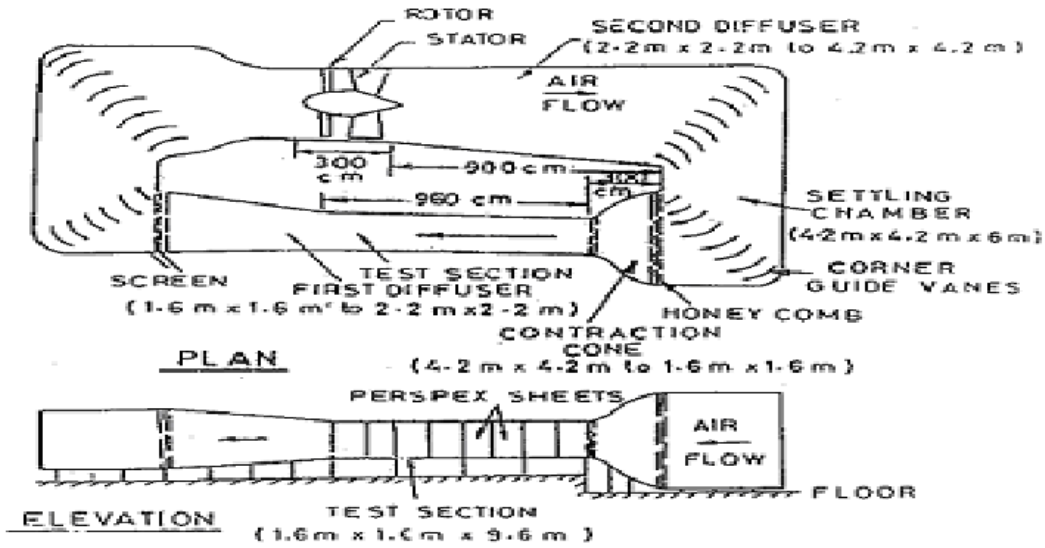


Figure 42: Plan and Elevation of the 1.6mx1.6m x9.6m Closed Circuit Wind Tunnel

The velocity profile for the tunnel can be given by power law as :

$$\frac{V}{V_0} = \left[\frac{z}{z_0} \right]^n \quad (11)$$

The values of n and z_0 depend on the roughness of the ground. To establish this relation, pitot tube was translated in vertical direction in line with axis of chimney to establish velocity profile in the tunnel, the power law exponent of the simulated boundary layer was found to be 0.182, which is in the acceptable range. The slight difference between the experimental velocity distribution and that specified by the code (IS 875 part 3, 1987) can be accounted for by including appropriate integral correction factors.

Given a velocity distribution $V(z)$ and chimney diameter variation, $D(z)$, the Bending Moment, $M(z_o)$ at the location z_o can be evaluated as:

$$M(z_o) = \int_{z_o}^H C_D \frac{1}{2} \rho V^2 D(z - z_o) dz, \quad (12)$$

We can define non-dimensional velocities and geometric parameters as,

$$V^* \equiv \frac{V(z)}{V_H}; \quad D^* \equiv \frac{D(z)}{H} \quad \text{and} \quad \eta \equiv \frac{z}{H}. \quad (13)$$

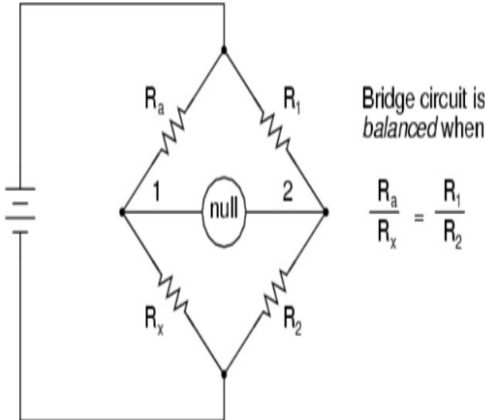
Where, V_H is the velocity at the top of the chimney. This allows us to express equation (12) as:

$$M(z_o) = \frac{1}{2} \rho C_D H^3 V_H^2 \int_{\eta_o}^1 V^{*2} D^*(\eta - \eta_o) d\eta \quad (14)$$

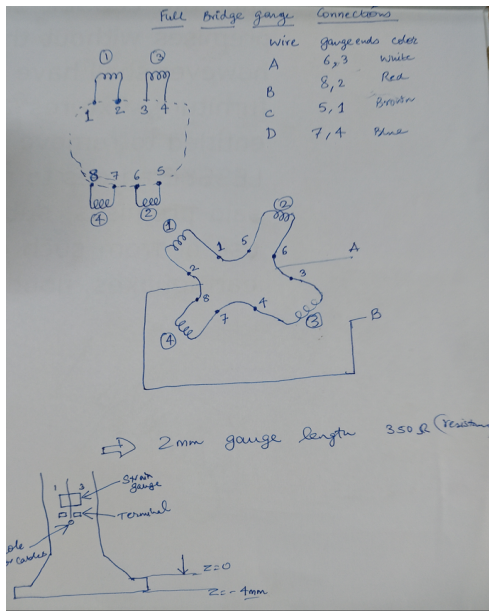
7.3 Strain gauge installation in full bridge arrangement

The Wheatstone bridge general arrangement can be shown below in Figure 43 (a) and the strain gauges are mounted in a similar fashion.

Figure 43 (b), shows the arrangement of all the 4 strain gauges in full bridge arrangement and also shows how they are located in a chimney with terminals and wires.



(a) Wheatstone bridge circuit



(b) circuit with gauges and color code

Figure 43: The calibration of weights on the chimney

The strain gauges were first glued to the primary surface through adhesives which show good bonding properties with the base material, this time we used permabond adhesive which shows good binding with high density polyethylene (HDPE), and then the terminals were glued and soldered with the strain gauge wires to complete the full bridge arrangement shown in Figure 43.

7.4 Details of instrumentation and data recording

Strain gauges were pasted on the external surface of the chimney model at four different heights along the chimney. At each height four 350Ω gauges were placed in two pairs 180° apart, so as to permit full-bridge operation. By properly aligning the chimney with respect to the flow direction, it is possible to determine the along-wind or across-wind response.

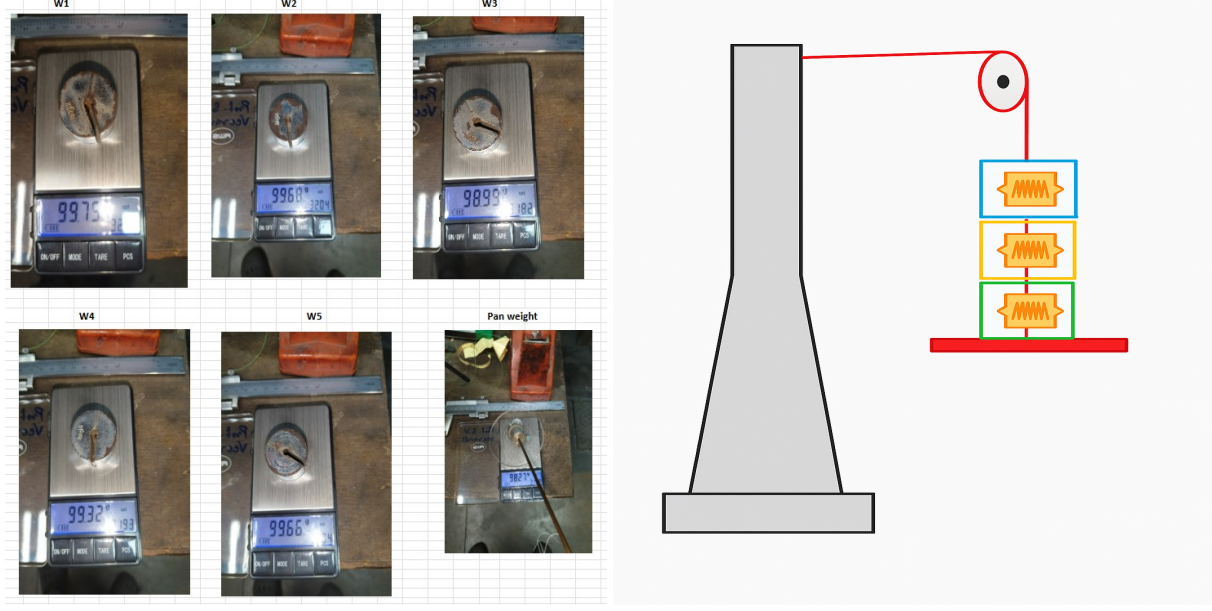
The outputs of the strain gauges were recorded using an NI USB-9237 strain data logger (24bit, 4 channel, simultaneous sample and hold, with a maximum throughput of 50k samples per second per channel).

During calibration approximately 24,000 samples were taken at 0.5k samples per second and averaged for every load. On the other hand, when the chimney was placed in the turbulent boundary-layer, approximately 80,000 samples (total record time of approximately 5 minutes) were recorded at 0.5k samples per second in every case.

These records were then processed to yield various statistics. The data was corrected for zero drift and noise, by recording the no-wind output of the strain gauges (approximately 16000 samples) before and after every data record. Since the data rate available is very high, it was not necessary to use an accelerometer while determining the natural frequency and damping ratio of the chimney model. Thus the loading error due to the accelerometer is not relevant here.

7.5 Calibration of gauges

known weights were used to calibrate the gauges response, in the below figures you can see the measured weights alongwith the pan and a diagram to shown how they were mounted on chimney.

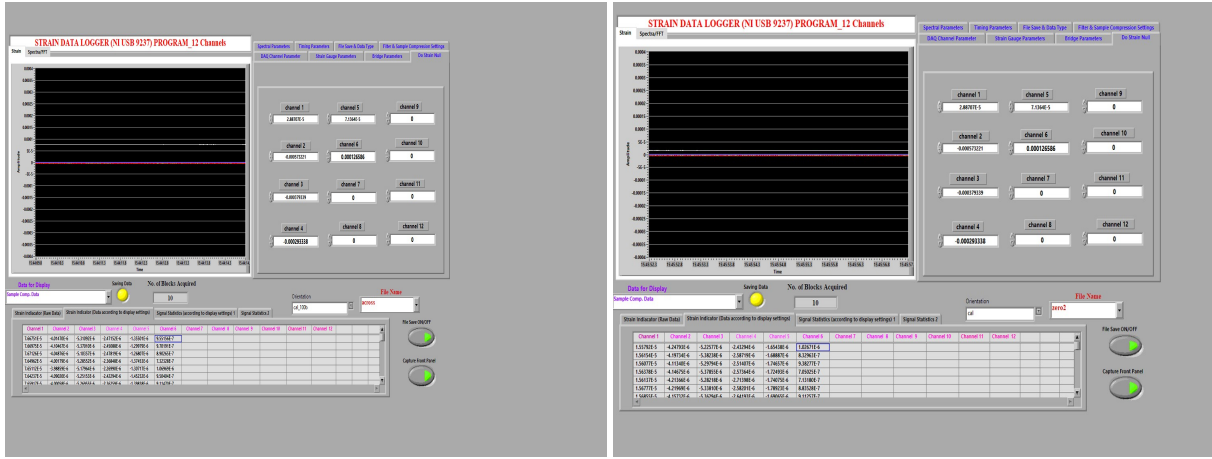


(a) Weights measured

(b) The calibration schematic

Figure 44: The calibration of weights on the chimney

The response of the calibrated weights was then measured for along and across orientations via the strain gauges and recorded in LabVIEW which can be seen below in Figure 45.



(a) Response with Pan

(b) Response after one weight is put

Figure 45: The response from gauges in LabView

7.6 Natural frequency and damping ratio experiment

Once we are done with calibration, the natural frequency response was calculated by tapping the HDPE chimney at the top along the four gauges, this was done by keeping in mind that multiple modes don't get excited and the structure should have a point contact with the tapping material. The recorded data from the strain gauges was taken to MATLAB for FFT to get the natural frequency shown in Figure 46.

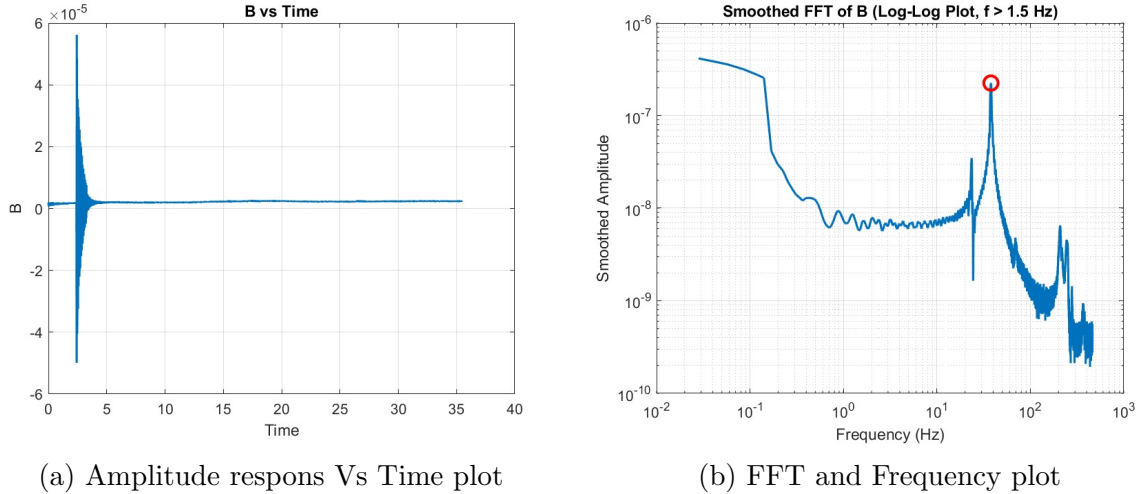


Figure 46: The response and Natural frequency

Figure 47 shows, the amplitude Vs Time response and for the calculation of damping ratio we would take amplitude decrement over a period of time (logarithmic decay)

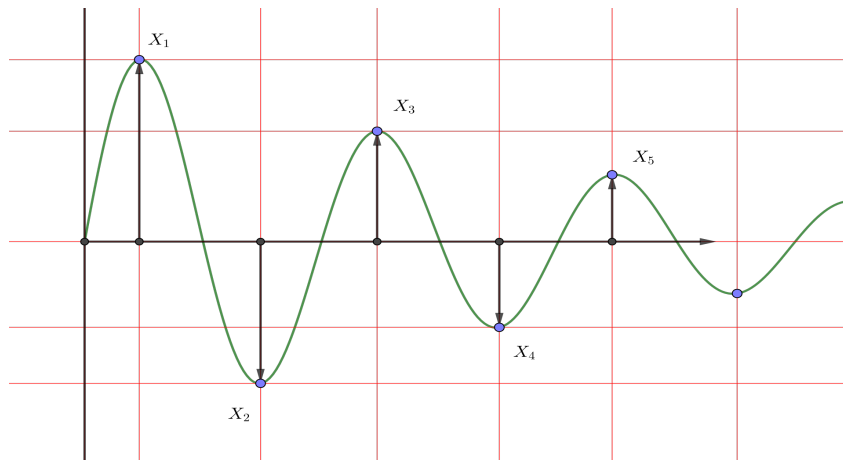


Figure 47: Amplitude Vs Time response

The formulation of decrement δ , is given in equation 15.

$$\delta = \frac{1}{n} \ln \frac{x(t)}{x(t + nT)} \quad (15)$$

Once we have the logarithmic decrement, we calculate the damping ratio for the data recorded, shown in equation 16.

$$\zeta = \frac{\delta}{\sqrt{4\pi^2 + \delta^2}} \quad (16)$$

7.7 Configurations for data recording

Different structures which are near the FGD chimney are constructed in proto scale and mounted in different angles in the wind tunnel, so as to get interference and data recorded for each case. We have turn-table, where we can directly rotate the structures in particular angles and outside turn-table we locate the exact co-ordinates for structures lying there before the recording starts.

The co-ordinates are given in GA drawing format to us, and we scale the distances keeping the FGD chimney as center.

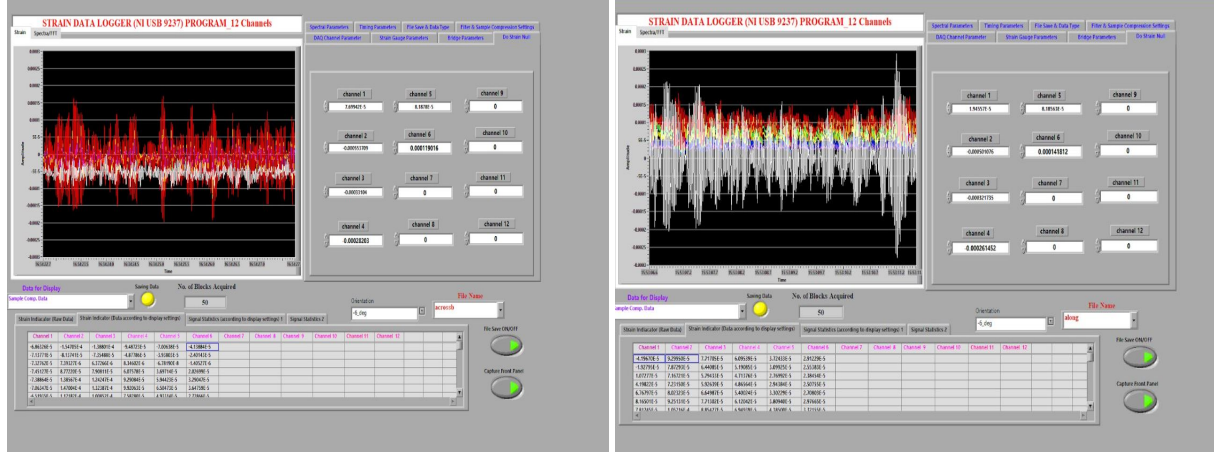
7.8 Result/Summary

The structures we mounted/fixed in different angles so as to capture the response in along and across wind, for capturing response on chimney. These recorded responses were then taken to calculate the bending moment and shear forces given in Section 7.2. Two such configurations are shown in below Figure 48



Figure 48: Two configuration for our experiment

The across(Figure 49a) and along(Figure 49b) wind responses from the gauges are shown in Figure 49. It can be confirmed while seeing these responses that only the gauges facing the wind show the drift while the gauge located at 90°, responds with zero mean.



(a) Across wind

(b) Along Wind

Figure 49: Responses of gauge in loaded condition

Finally we calculate with the responses for each angle, the bending moment and shear forces and tabulate them for seeing the worst-case scenario.

We can also find the worst maxima in bending moment and shear forces in orientation and wind direction from this table in Figure 50.

Orientation	BASE BENDING MOMENT (NM)						BASE SHEAR (N)					
	Along		Across		SRSS		Along		Across		SRSS	
	Shell	Completed	Shell	Completed	Shell	Completed	Shell	Completed	Shell	Completed	Shell	Completed
Isolated	9.19E+07	9.51E+07	1.89E+07	2.18E+07	6.03E+07	6.31E+07	1.51E+06	1.56E+06	2.56E+05	3.00E+05	9.73E+05	1.01E+06
0	8.28E+07	8.79E+07	3.16E+07	2.47E+07	6.05E+07	6.00E+07	1.35E+06	1.52E+06	5.56E+05	4.45E+05	1.01E+06	1.05E+06
10	7.77E+07	7.97E+07	2.94E+07	2.34E+07	5.66E+07	5.49E+07	1.26E+06	1.36E+06	5.07E+05	4.43E+05	9.34E+05	9.55E+05
20	8.37E+07	8.28E+07	4.00E+07	3.02E+07	6.57E+07	5.97E+07	1.37E+06	1.41E+06	7.03E+05	5.19E+05	1.10E+06	1.02E+06
30	8.69E+07	8.25E+07	3.95E+07	3.22E+07	6.70E+07	6.06E+07	1.45E+06	1.41E+06	6.33E+05	5.54E+05	1.10E+06	1.04E+06
40	8.21E+07	9.15E+07	4.80E+07	4.52E+07	7.01E+07	7.27E+07	1.34E+06	1.57E+06	9.02E+05	9.03E+05	1.23E+06	1.33E+06
50	8.85E+07	9.69E+07	4.30E+07	4.65E+07	6.99E+07	7.62E+07	1.51E+06	1.68E+06	8.60E+05	9.27E+05	1.27E+06	1.40E+06
52	9.61E+07	9.94E+07	3.77E+07	4.57E+07	7.07E+07	7.69E+07	1.44E+06	1.41E+06	5.59E+05	6.55E+05	1.06E+06	1.10E+06
60	8.73E+07	9.48E+07	3.73E+07	5.09E+07	6.60E+07	7.79E+07	1.73E+06	1.75E+06	6.45E+05	8.63E+05	1.25E+06	1.39E+06
70	5.11E+07	6.48E+07	3.27E+07	5.07E+07	4.57E+07	6.48E+07	8.34E+05	1.13E+06	5.20E+05	8.26E+05	7.35E+05	1.08E+06
80	8.01E+07	9.46E+07	3.16E+07	3.53E+07	5.90E+07	6.87E+07	1.33E+06	1.56E+06	4.81E+05	5.00E+05	9.59E+05	1.09E+06
82	9.29E+07	1.04E+08	3.10E+07	4.00E+07	6.56E+07	7.62E+07	1.54E+06	1.62E+06	4.57E+05	5.91E+05	1.06E+06	1.17E+06
84	1.00E+08	1.14E+08	3.97E+07	4.52E+07	7.41E+07	8.44E+07	1.55E+06	1.79E+06	6.17E+05	6.65E+05	1.14E+06	1.30E+06
86	9.94E+07	1.06E+08	3.61E+07	4.57E+07	7.17E+07	8.05E+07	1.59E+06	1.62E+06	5.52E+05	6.88E+05	1.13E+06	1.22E+06
-10	8.47E+07	8.15E+07	4.09E+07	3.28E+07	6.67E+07	6.04E+07	1.38E+06	1.41E+06	6.58E+05	5.46E+05	1.08E+06	1.04E+06
-20	8.26E+07	8.22E+07	4.41E+07	3.14E+07	6.78E+07	6.01E+07	1.35E+06	1.43E+06	7.93E+05	5.47E+05	1.15E+06	1.04E+06
MAXIMA	1.00E+08	1.14E+08	4.80E+07	5.09E+07	7.41E+07	8.44E+07	1.73E+06	1.79E+06	9.02E+05	9.27E+05	1.27E+06	1.40E+06

Figure 50: Bending moment and Shear force